Macromolecular Materials and Engineering
www.mame-journal.de

Management of Operational Parameters and Novel Spinneret Configurations for the Electrohydrodynamic Processing of Functional Polymers

Pedro M. Silva, Sergio Torres-Giner, António A. Vicente, and Miguel A. Cerqueira*

Functional materials have become key drivers in the development of multiple high-end technologies. Electrohydrodynamic processing (EHDP) is a straightforward method to generate polymer micro- and nanostructures that can be applied to the food, pharmaceutical, environmental, and biomedical areas, among others, since these can yield materials with higher performance. Some of the EHDP's advantages over other polymer processing technologies rely on its high versatility, by which the final assembly can be modified in different ways to combine materials with multiple properties and also in different morphological structures, and the use of room processing conditions, meaning that thermolabile ingredients can be incorporated with minimal activity loss. This review provides the historical background, process basics, and the state-of-the-art of the most recent advances achieved in the EHDP technology dealing with the control of its operational parameters to optimize processability and achieve end-product quality and homogeneity. It also focuses on the newly developed modes of operation and spinneret configurations that can lead to the formation of a wide range of micro- and nanostructures with different functionalities and solve some of its current technical limitations. Finally, it also further highlights the potential applications of the resultant hierarchical functional polymer-based materials obtained by these novel EHDP methods.

1. Historical Overview

Electrohydrodynamic processing (EHDP) is regarded as a novel technique to produce polymer micro- and nanostructures. Nevertheless, the electrohydrodynamic concept is not new and it can be traced to the late 19th century and the beginning of the 20th century with the first observations and descriptions of the basics. These previous experiences would, in time, allow for the creation of EHDP equipment, coming by Rayleigh in 1882,[1] and more extensively studied by Zeleny in 1914.[2,3] The first practical applications of EHDP, in the form of an electrospinning equipment for the preparation of non-woven threads for the textile industry, came in 1934 when Anton Formhals first patented a process for the preparation of artificial threads.[4] However, the initial patent faced some problems (e.g., inadequate drying of fibers in the collector) that were later improved upon in a second patent in 1939.[5] Following patents by Formhals focused on fiber optimization (e.g., length, strength, and production of composites).[6,7] Later, in the 1950s and 1960s, Vonnegut and Taylor, respectively, studied in-depth the effects of electrical fields on liquid droplets that resulted in the generation of micro-particles through atomization.[8] In particular, Vonnegut and Neubauer demonstrated that it was possible to produce a stream of highly electrified droplets of small diameter (≈0.1 mm) through the application of 5–10 kV potentials to liquids in small capillaries, being one of the first demonstrations of electrical atomization.[8–10] Then, Taylor studied and improved upon Zeleny's works and first modeled and described mathematically the shape of the formed jet at the tip of electrified capillaries, the conical interface that was named "Taylor cone."[9,10] Still, EHDP was at large ignored until the 1990s, when researchers paid attention to the potential of nanotechnology in several areas and started to look for new technologies to produce ultrathin structures for different applications.

EHDP has shown increasing interest throughout the last three decades. **Figure 1** gathers information on the EHDP publications through time, type of publication, country, and research field. In particular, it can be observed in Figure 1a that research on EHDP increased exponentially in the 1990s, a trend that can be seen up to these days, as a result of both the increasing knowledge and interest in nanotechnology/nanostructures and the advantages resulting from using this technique for the production of micro- and nanostructures in place of other frequently used techniques.[11–13] It is also noteworthy that an overwhelming ma-

P. M. Silva, M. A. Cerqueira
International Iberian Nanotechnology Laboratory (INL)
Avenida Mestre José Veiga, Braga 4715-330, Portugal
P. M. Silva, A. A. Vicente
Centre of Biological Engineering
University of Minho
Campus de Gualtar, Braga 4710-057, Portugal
S. Torres-Giner
Research Institute of Food Engineering for Development (IIAD)
Universitat Politècnica de València (UPV)
Camino de Vera s/n, Valencia 46022, Spain
E-mail: storresginer@hotmail.com

The ORCID identification number(s) for the author(s) of this article can be found under https://doi.org/10.1002/mame.202100858

DOI: 10.1002/mame.202100858

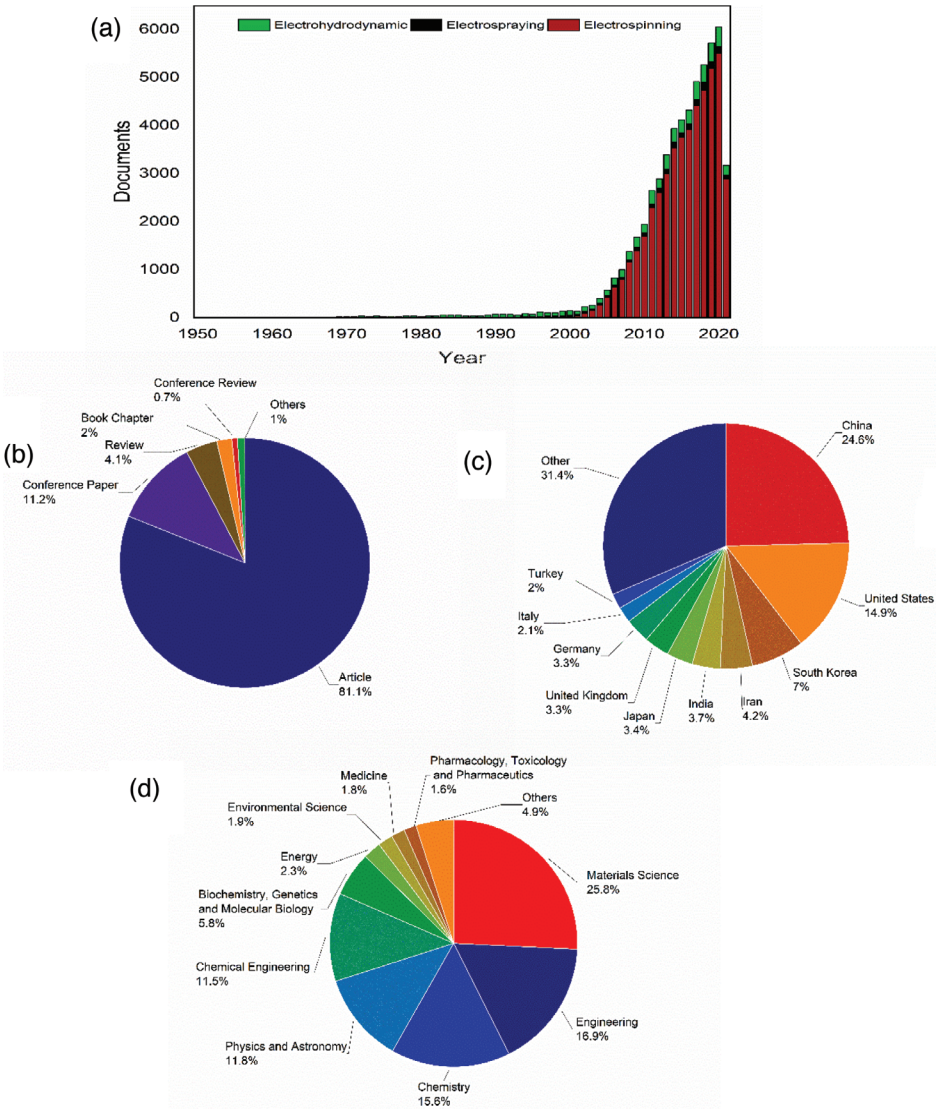

Figure 1. Scopus data regarding EHDP publications across time (a) and gathered by type of b) publication, c) country, and d) subject area. Data taken on June 11, 2021. Keywords used: "electrospinning", "electrospun", "electrohydrodynamic", "electrospraying", or "electrosprayed."

jority of publications regarding EHDP are from original research papers (more than 80%, see Figure 1b). Moreover, these research efforts have been conducted worldwide, with more than 150 research centers or universities spread out by over 130 countries (see Figure 1c). As it can be seen in Figure 1d, areas range from material science to chemistry and agricultural and biological sciences. Most of them are in the field of materials science (25.8%), engineering (16.9%), and chemistry (15.6%).

2. EHDP Basics

Studies on EHDP vary in their focus, with some studies dealing with the process itself, others reporting the relationship between parameter influence and obtained structures, as well as studies that focus on the optimization and characterization of the produced structures.[11–20] This increase in research has fostered advances in different areas such as biomedicine, environmental protection, bioengineering, pharmacologic, materials, food, among others, demonstrating the versatility of EHDP, both regarding the technology and the materials that can be used.[14–16,21,22] Another proof of the EHDP versatility is the reported use of hundreds of polymers to produce micro- and nanostructures using this technology. Such materials range from simple polymers to complex composites, including synthetic and natural polymers, biodegradable and non-biodegradable, and their blends. The reported materials used to produce fibers or particles by EHDP include, for instance, piezoelectric polymers for the fabrication of nanofiber scaffolds in tissue engineering,[23] biopolymers for the encapsulation of bioactive compounds for use in the food industry,[15] fluorescent polymers for application in nanofiber optical sensors,[24] and composite polymers to be applied in the preparation of nanotubes for engineering applications.[17]

In general terms, EHDP is a facile top-down method to produce micro- and nanostructures.[25,26] It can be operated in two basic methods: electrospinning, which allows produc-

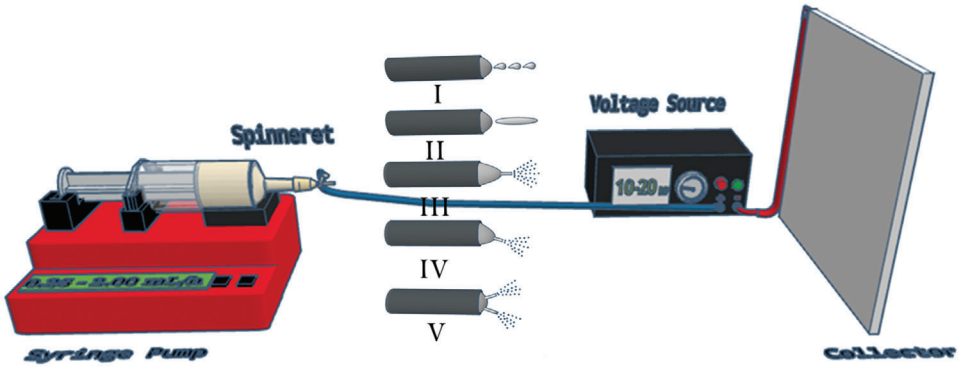

Figure 2. Schematic illustration of the basic setup of EHDP with schematic illustrations of electrospinning and electrospraying modes: I) micro dripping; II) spindle; III) cone jet; IV) oscillating jet; and V) multiple jet.

ing micro- and nanofibers, and electrospraying that produces micro- and nanoparticles. Operation methods and equipment may vary according to the intended structures and use, but the basic setup is equal for both electrospinning and electrospraying techniques.[12,25–29] A schematic illustration of the basic setup of EHDP, both for electrospinning and electrospraying, can be seen in **Figure 2**. A basic setup requires just four components, namely a syringe equipped with a metal capillary (usually a needle-shaped spinneret), a feed pump to feed the polymer solution through the spinneret, a high-voltage power supply (usually applied at the tip of the spinneret), and a grounded collector (of variable morphology) to collect the produced structures.[12,25–29] The voltage difference between the spinneret and the grounded collector creates an electrical field that, when the droplet's surface tension is exceeded, draws the polymer solution from the spinneret tip to the grounded collector, either in the shape of fibers (electrospinning) or particles (electrospraying). This causes rapid evaporation of the solvent and results in the production of dry micro- and nanofibers or micro- and nanoparticles, respectively, that are deposited on the collector.[11,25,27,29]

The electrospinning of polymer-based solutions can be easily obtained using the basic setup. The electrospinning process is conducted in three steps: jet initiation, elongation, and solidification. In order to achieve this, it is necessary to firstly polarize the polymer solution through the application of a high-voltage potential, which leads to the formation of the so-called Taylor cone. Then, when the applied electrical field is above the surface tension of the polymer solution, jet initiation and elongation occur.[11,30–32] The jet elongates due to the shearing of the viscoelastic solution and bending and whipping motions. As jets are ejected from the tip, a rapid evaporation of solvent takes place, leading to the solidification of the fibers on the grounded collector. The bending and whipping motions are essential to this rapid evaporation as they allow for an extensive reduction of the jet.[11,30–32] A steady state is obtained when the flow-rate producing the Taylor cone equals the flow-rate of the ejected solution. This steady state occurs in limited conditions when the appropriate solution and processing parameters are used. Outside of a steady state, the polymer solution is at risk of breaking into droplets ("Plateau–Rayleigh instability"), leading to the formation of "broken" fibers.[11,30–32]

Electrospraying utilizes the same principles of electrospinning. An electric field is similarly applied between the spinneret and the grounded collector but, in the case of electrospraying, polymer solutions with lower viscosity are used. Thus, the jets expelled from the Taylor cone are disrupted due to the varicose instability caused by the low viscoelasticity of the polymer solution.[12,15,32] This disruption transforms the ejected jets into droplets instead of fibers. The charged droplets are subsequently broken up into smaller and stabler droplets due to Coulombic fission. Indeed, the Coulombic fission and repulsion between the charged droplets prevent their agglomeration, leading to a rapid solvent evaporation and the solidification of micro- and nanoparticles on the metal collector.[28,31]

However, the development of a Taylor cone occurs in a limited set of operating conditions and, as such, changes to these conditions can lead to the development of different modes of spinning and spraying cones. These different modes, also identified in Figure 2, were first categorized by Cloupeau and Prunet-Foch in the 1990s,[33,34] and include the following ones: I) dripping or micro dipping (usually due to low voltages); II) spindle mode, as the applied voltage increases; III) steady cone-jet mode, in which the appropriate voltage is being applied; IV) oscillating jet mode, which occurs when the steady cone jet mode shifts laterally due to a slight voltage increase; and, as voltages increase, it can turn into the V) multi-jet mode since the excess voltage creates multiple cones.[33–35]

Although EHDP is versatile, adaptable, and facile to use, there is no generic or common EHDP apparatus ideal for all types of polymers and intended applications.[11,15,25,27] Therefore, the final results (e.g., fibers or particles, with their intended morphology or size) are dependent on several parameters related either to the process (e.g., flow-rate, voltage, and tip-to-collector distance), solution properties (e.g., viscosity, surface tension, and conductivity), and ambient conditions (e.g., temperature and relative humidity).[11,15,25,27]

3. Operational Parameters

EHDP is regarded as a simple technique to produce micro- or nanoparticles and fibers with reproducible morphology and size distribution of a narrow range. Despite that fact, when the goal is to produce very specific particles or fibers, this process can

turn into a challenge. As previously mentioned, there are many parameters that can influence the behavior of EHDP, most of which are inter-dependent and must be taken into consideration when setting up these experiments. These parameters can be classified into three categories: solution properties, process parameters, and ambient conditions.[14,18,36,37] Solution properties include viscosity, which depends on the molecular weight (M_W) of the polymer as well as the polymer solution concentration, the solvent type, namely its volatility, the surface tension, and conductivity.[14,18,36,37] Process parameters include applied voltage or electric field, the feed flow-rate of the polymer solution, the spinneret morphology (type of spinneret and diameter), collector morphology, and the distance between the spinneret tip and the collector.[14,18,36,37] Additionally, ambient conditions, such as temperature and relative humidity, can also affect the result of EHDP.[14,18,36,37]

The management of these operational parameters can be crucial to optimize the fabrication of different polymer micro- and nanostructures by EHDP. The discussion of the different operational parameters is presented below, gathering in **Table 1** a summary of their influence on EHDP.

3.1. Solution Properties

Polymers' M_W, solution concentration, and viscosity are intertwined parameters that have a high influence on the type of structure that is obtained during EHDP. With increasingly higher values in these parameters, it is more likely to obtain fibrous structures than particles, which are typically obtained with low-M_W polymers and at lower concentrations and viscosities. This is due to an increase in chain entanglements that occurs with the increase in M_W and polymer concentration.[36] Chain entanglements are the physical interlocking of polymer chains (chain overlapping), which are higher in high-M_W polymers and, consequently, lower in low-M_W ones. In a polymer solution, the number of chain entanglements is also affected by the concentration or volume fraction ($\varnothing_p$).[38] The solution entanglement number [$(n_e)_{soln}$] can be determined using Equation (1), which is essential to determine whether fibers or particles will be obtained during EHDP.[38] It is defined as the ratio between polymer's M_W to its solution entanglement molecular weight [$(M_e)_{soln}$], where M_e is the entanglement molecular weight of the undiluted polymers:[26,38]

$$(ne)_{soln} = \frac{M_W}{(M_e)_{soln}} = \frac{(\phi_P M_W)}{M_e} \quad (1)$$

Polymer concentration and M_W are connected to the resultant viscosity of the solution. At certain polymer concentrations, the viscosity of a solution changes abruptly, a point that can be classified as the overlap concentration, that is, c^*. In dilute solutions (below the critical value c^*, typically $c << c^*$) no chain entanglement exists and, therefore, electrospraying typically occurs due to the varicose instabilities affecting the polymer jet. As concentration increases ($c \sim c^*$), chain overlap is initiated, and a mixture of fibers and beads is habitually observed. At higher concentrations of polymer ($c > c^*$), chain entanglements can stabilize the electrospinning jet and, thus, allow for solvent evaporation and fiber formation.[26,38] By establishing a relationship between particle or fiber formation and the value of $(n_e)_{soln}$, the spinnability of a given solution can be determined. For instance, Shenoy et al.[38] showed that, generally, $(n_e)_{soln} < 2$ (dilute regime) results in electrospraying, values of $(n_e)_{soln}$ between 2 and 3.5 (semi-dilute unentangled regime) leads to the electrospinning of beaded fibers, while $(n_e)_{soln} > 3.5$ (semi-dilute entangled regime) yields the electrospinning of smooth fibers.[38] Similar ranges of values for the solution entanglement number have been found in previous works.[39] Shenoy et al.[38] also reported that, for low-M_W polymers, electrospinning might not be possible due to lower relaxation or disentanglement time. In this regard, Correia et al.[40] tested the impact of polymer concentration in the morphology of the produced microstructures. To this end, poly(vinylidene fluoride) (PVDF) solutions were prepared between 2% and 10% (w/v) and the performed morphological analysis showed that no spherical particles were obtained at low concentration, that is, 2% (w/v), while at the intermediate concentration of 5% (w/v) spherical particles were produced. Finally, at high concentrations of 7 and 10% (w/v), particles, as well as fibers, were formed. Therefore, an increase in the concentration of PVDF was reported to lead to the successful production of smooth and bead-free fibers. In another study, Silva et al.[26] evaluated the impact of the concentration of hydroxypropyl methylcellulose (HPMC) in EHDP for the production of different structures. Low- and high-M_W HPMC contents were tested, ranging in concentrations from 1% to 6% (w/w), and 1 to 2.5% (w/w), respectively. Low-M_W HPMC led to the formation of rod-like and round particles, while high-M_W HPMC yielded the formation of beaded and bead-free fibers. The particle diameter varied between 833 and 1188 nm, whereas the aspect ratio ranged between 1.3 and 3.7. The resultant nanofibers displayed a mean diameter ranging between 79 and 161 nm.

The solvent is another key parameter that influences EHDP and a great variety of solvents can be selected. Solvent selection is intertwined with surface tension (a critical parameter for the formation of the Taylor cone), conductivity, and evaporation rate (volatility) during the path from the spinneret to the collector. Surface tension and solvent volatility must be within an adequate range or able to be modified in order to ensure the solvent can be used as a electrospinnable solution. The miscibility between a solvent and the desired polymer also affects the type of structure obtained. Generally, good solubility values of the polymer in the solvent might lead to the formation of particles, as viscosity will be lower, while less soluble pairings of solvents and polymer might lead to higher viscosities, resulting in the formation of fibers.[14,42,43] Decreasing surface tension is a critical step in order to be able to form a Taylor cone at the tip of the spinneret and allow the ejection of particles or fibers. One of the ways to achieve this is to add surfactants to the solution. These additives cannot only affect surface tension values, but might alter conductivity and viscosity as well. In this regard, Fang et al.[44] studied the impact of different surfactants on the electrospinnability of lignin. Authors demonstrated that, by increasing the amount of surfactant used, the conductivity increased while surface tension decreased, and viscosity varied according to the type of surfactant used. An initial addition of surfactant, such as dodecyltrimethylammonium bromide (DTAB) and a non-ionic surfactant, TritronTX-100, led to the pro-

Table 1. Influence of experimental parameters on EHDP.

Category	Parameter	Influence on electrohydrodynamic processing	Ref.
Solution parameters	Polymer molecular weight (M_W), concentration, and viscosity.	Low-M_W polymers induce lower solution viscosities that, in turn, are more likely to form particles. On the contrary, polymers with higher M_W are more likely to form fibers due to an increase in the solution viscosity. These are due to low and high chain entanglements, respectively. Increasing polymer concentration (and therefore viscosity) leads to a transition from particle formation to beaded fibers to bead-free fibers. At low viscosities, particles are formed due to varicose instability while, at high viscosities, the electrospinning jet can be stabilized and produce fibers.	[38–41]
	Solvent	Solvent choice can affect viscosity, surface tension, and conductivity. Appropriate solvents have low but sufficient surface tension, adequate solubility of the polymer, and relatively low volatility, allowing for solvent evaporation and structure deposition on the collector. Extremely high solvent volatility is linked to porous surface morphology and needle clogging, whereas excessive low volatility impairs solvent evaporation during the process and affects fiber formation.	[14,42,43]
	Surface tension	Overcoming surface tension is essential to conduct EHDP. A minimal surface tension is required to avoid process instabilities. Low surface tension solutions require less voltage, while higher surface tension solutions require more voltage or are not spinnable. Surface tension can be modified through the addition of surfactants.	[36,42,44,45]
	Conductivity	Solutions with higher conductivity tend to form jets of higher charge, producing smoother structures (e.g., round-like beads or bead-free fibers) with lower diameters. However, excessive conductivity can disrupt the balance between charge droplets and applied voltage, leading to jet instability and morphology changes (e.g., higher diameters and deformed structures).	[41–43]
Process parameters	Applied voltage	This process parameter is essential to overcome surface tension. High applied voltages can lead to structures with lower diameters due to size reduction of the fluid jet, but can also cause particle elongation in electrospraying. Excessive voltage leads to destabilization of the Taylor cone, leading to the formation of structures with higher diameters and broader size distribution.	[40,41,46,47]
	Flow-rate	Low rates are more adequate in electrospraying processes, producing more spherical particles. Using high rates can lead to the production of beaded fibers or lead to incomplete solvent evaporation, resulting in merged particles and fibers. A steady state is achieved when the feed flow-rate equals the flow-rate of the ejected solution. Flow-rate is the main parameter affecting fiber and bead throughputs.	[40,41,47]
	Spinneret morphology	Conflicting reports regarding the influence of needle diameter exist, but it has been shown that needle diameter affects the size and stability of the Taylor cone. Lower diameters can cause needle blockage in electrospinning and are more typically used in electrospraying, where lower viscosity solutions are used.	[40,47]
	Tip-to-collector distance	It is very intertwined with applied voltage: As tip-to-collector distance increases, so does the voltage requirement in order to maintain a stable Taylor cone. Using inadequate distances may lead to incomplete solvent evaporation, resulting in particle and fiber merge in the collector.	[41,47]
Ambient parameters	Relative humidity	Depending on the polymer used, relative humidity can increase, decrease, or not affect particle or fiber diameter and morphology. High values of relative humidity are known to lead to the development of porous structures. Extremely high humidity conditions can make a polymer non-spinnable through the decrease in electrostatic charges at the tip of the spinneret.	[43,45,48,49]
	Temperature	Lower temperatures increase the viscosity of polymers, leading to higher diameter and size distributions. Higher temperatures have the inverse effect. Excessively high temperatures can have a negative effect on the diameter of the structures due to an increase in solvent evaporation.	[50,51]

duction of smooth fibers, but the continuous addition of surfactant led to the formation of beaded fibers. For the third surfactant (sodium dodecyl sulfate, SDS), the opposite effect was verified with the continuous addition of this additive since smoother fibers were obtained. The authors observed that the critical micelle concentration of surfactants greatly influenced the modulation of the polymer solution and the morphology of nanofibers. In another study, Topuz et al.[43] assessed the effect of conductivity on the spinnability of polymers of intrinsic microporosity (PIM) by means of the addition of salts. Mostly, higher concentrations of PIM-1 in 1,1,2,2-tetrachloroethane (TeCa) were required to produce bead-free fibers. It was observed that the addition of an ammonium salt increased the conductivity of the solution and greatly improved its spinnability, yielding bead-free fibers. As opposite, without the addition of the ammonium salt, electrosprayed particles and droplets were observed.

3.2. Process Parameters

The applied voltage is a critical parameter for EHDP since without voltage no Taylor cone is obtained. Therefore, the applied voltage should be enough to develop a Taylor cone, allowing for electrospinning or electrospraying to occur. As mentioned above, typically, with an increase in voltage, different jet modes can be obtained though, ideally, EHDP occurs in the cone jet mode.[33–35] The applied voltage may also influence the morphology of produced particles and fibers.[46] The electrical field of a certain system is not only a function of the applied voltage, but also of the tip-to-collector distance. Typically, the closer the distance, the lower the voltage requirements, which is one of the core principles of electrohydrodynamic jet printing, and vice-versa. Tip-to-collector distance is also essential in ensuring that the expelled jet from the spinneret has enough time of flight until reaching the collector to evaporate the solvent and obtain uniform micro- and nanostructures. Otherwise, droplet splashing of polymer solution and particle and fiber merging will occur, altering the morphology of the structures.[36,37]

The spinneret morphology influence on needle electrospinning or electrospraying spinnerets is controversial. Some reports state that it does not affect the diameter of fiber or particle, while some other reports state that it can affect fiber or particle diameter. Nevertheless, it has been accepted that needle diameter affects the stability of the Taylor cone. Typically, smaller diameters are more frequently used for the formation of micro- and nanoparticles as lower viscosity solutions are used. However, when using solutions with higher viscosities, it is possible to have a blockage of needles with low diameters.[40,47]

Furthermore, feed flow-rates can have a great impact on the morphology of the structures obtained from EHDP since it affects the transfer rate and jet speed. In addition, due to the relationship with the tip-to-collector distance, jets produced by higher flow-rates might not have enough time of flight to the collector for solvent evaporation, leading to the deposition of merged fibers and particles.[40,41] As previously mentioned, the feed flow-rate should be equal to the flow-rate of the ejected solution in order to maintain a steady state.[32] In this context, Correia et al.[40] tested the influence of several parameters on the morphology of electrosprayed particles based on PVDF, namely flow-rate and applied voltage. Flow-rate values varied between 0.2 and 4 mL h^{-1}, while voltage ranged between 15 and 25 kV and the tip-to-collector distance was fixed at 20 cm. Results showed that low flow-rate values were more adequate since these produced microparticles with lower diameters and a uniform morphology, while higher values produced particles with higher diameters and a less uniform particle morphology due to particle agglomeration in the collector. Since more polymer solution is available at the tip of the spinneret with higher feed flow-rates, this results in the ejected polymer jet having less time to evaporate the solvent, causing aggregation of particles. By varying the applied voltage, Correia et al.[40] noticed that particles at higher voltages were less uniform in terms of morphology, with particles suffering elongation and the presence of some fibers. On the contrary, at lower voltages, more spherical particles were obtained. These results demonstrate the effect of voltage on the particle or fiber morphologies and the need for voltage optimization during EHDP.

In this sense, Zhou et al.[46] studied the effect of voltage on the morphology of nanofibers using a modified coaxial electrospinning setting using HPMC and ketoprofen, as the core fluid, and ethanol, as the sheath fluid, demonstrating the positive effect of voltage in the reduction of the nanofiber diameters. A modified coaxial electrospinning process was used in order to avoid clogging, minimize ambient interferences, control solvent evaporation rate from the core fluid, and increase the spinning time (as a function of reduced clogging). It was further observed that in single fluid electrospinning, the effect of voltage was not very significant. In the previous study of Topuz et al.,[43] dealing with coaxial electrospinning, voltage proved to be important since fiber diameters varied between 870 and 540 nm for applied voltages ranging from 13 to 16 kV. This demonstrated the potential of using modified coaxial electrospinning techniques to control the diameter of the produced nanofibers. By increasing the voltage, smaller Taylor cones were obtained, reducing the size of the fluid jet and, thus, the diameter of the nanofibers. Nevertheless, other studies have shown that an excessive increase of voltage can lead to destabilization of the Taylor cone that, in turn, yields polymer structures with higher diameters. For instance, Jain et al.[47] demonstrated that electrosprayed polyethylene glycol-based (PEG) hydrogel microparticles, produced at 10 and 12 kV, displayed similar diameters, around 100 μm. However, when the voltage was increased to 25 kV, diameters increased to 150 μm. Moreover, it was observed an increase in the size distribution for the particles formed at 25 kV, resulting from the destabilization of the Taylor cone.

In terms of process parameters, Smeets et al.[41] performed a comprehensive study on the effect of polymer concentration, conductivity, flow-rate, applied voltage, and tip-to-collector distance on the electrospraying of several polymers, with a specific focus on the established cone jet. Results showed that, for some of the explored polymer-solvent combinations, an increase of viscosity led to a transition from electrospraying (formation of particles) to electrospinning (formation of fibers). Regarding conductivity, when solution conductivity was increased to upper limits, no spraying cone was visualized. When increasing the feed flow-rate, only low conductivity solutions were able to produce a spraying cone, signaling that high conductivity liquids have higher charges and create a more unstable electrospraying process. Regarding process parameters, it was shown that higher tip-

to-collector distances and higher voltages were more successful in producing stable spraying cones. It was also demonstrated that larger tip-to-collector distances require higher voltages, as one would expect. Regardless of tip-to-collector distance, low flow-rates were more successful in obtaining stable spraying cones while, oppositely, high flow-rates required higher applied voltages. This observation confirms the above-described findings regarding solvent evaporation at higher feed flow-rates.

3.3. Environmental Conditions

In addition to the solution properties and process parameters, the environmental conditions under which the particles and fibers are prepared also influence the success of EHDP and the final morphology and size of the obtained structures. Temperature changes can lead to different viscoelastic behaviors and solvent evaporation rates, while changes in the relative humidity must be carefully controlled due to these can influence the electrostatic field.[14,36,50,51] For example, Wang et al.[50] assessed the temperature effect on the size and size distribution of chitosan microparticles by electrospraying, testing temperatures ranging from 25 to 50 °C. It was found that the viscosity of the chitosan solution decreased for higher temperatures, which led to a decrease in both the diameter and size distribution of the microparticles, creating a more uniform process at high temperatures. Nevertheless, the authors also noted that, when increasing the temperature to 50 °C, the mean diameter increased (when compared to 40 and 45 °C) and that surface morphology was affected with some particles losing their spherical shape. Guang et al.[51] also studied the influence of temperature, in the 20–80 °C range, on the production of polyacrylonitrile (PAN) nanofibers. Authors noted that an increase in temperature led to lower viscosity and surface tension values, which in turn yielded a decrease in the mean fiber diameters. However, it was also observed that an excessive increase in temperature yielded a higher solvent evaporation rate of the polymer solution, leading to an early termination of the stretching of polymer jets. This environmental change thus resulted in higher fiber diameters, confirming that temperature can have a positive effect on the decrease of fiber diameter, but the use of excessively high temperatures can also exert a negative effect.

The effect of relative humidity can also be dependent on the type of polymer since some polymers are more stable to moisture variations than others.[45,48,49] For instance, Topuz et al.[43] studied the effect of relative humidity on the spinnability of PIM-1 and found that, while neither fiber mean diameter or morphology were significantly affected, the production yield of fibers was diminished at high values. The observed effect was attributed to the loss of charge in the spinning head. Pelipenko et al.[48] similarly evaluated the influence of relative humidity on several polymers, such as poly(vinyl alcohol) (PVA), a blend of PVA and hyaluronic acid, poly(ethylene oxide) (PEO), and a blend of PEO and chitosan. It was concluded that, at low relative humidity values, thicker nanofibers were obtained, which was attributed to rapid solvent evaporation. However, at high values, the solvent evaporation was slower, resulting in thinner fibers. Furthermore, Yazgan et al.[45] also showed that, by increasing relative humidity, the mean fiber diameters of electrospun fibers made of a blend of polystyrene (PS) and polyvinylpyrrolidone (PVP) increased. It was also noted that at high relative humidity values, the surface morphology of the fibers changed, becoming more porous than at low values. Huang et al.[49] noticed the same effect on the morphology of electrosprayed microparticles of polymethylmethacrylate (PMMA). It was reported that the mean particle diameter remained constant across a range of relative humidity values, while morphology changed for microparticles prepared at higher values, also displaying increased porosity. These results show that relative humidity should be carefully controlled in order to obtain the desired morphology of the produced structures.

Therefore, solution properties, process parameters, and ambient conditions can have a great influence on the final micro- and nanostructures obtained by EHDP. Furthermore, by controlling these parameters, it is possible to develop the right morphology according to the selected targeted application. These parameters are highly interconnected and the recommendations described above can serve as the basis for selecting the right operational conditions. It can also be relevant for choosing the appropriate initial conditions for novel polymer-solvent systems, where future works should certainly consider and deal with the combination of these parameters.

4. Spinneret Configurations

Current methods of operation or spinneret configurations for electrospinning and electrospraying evolved from the basic mode, described in previous Section 2, to new and more complex setups. These novel configurations will allow the production of polymer micro- and nanostructures with functional properties and/or solve some of the particular process disadvantages (e.g., low production yield) of EHDP. The main new configurations with their operation modes are listed, along with their respective advantages and drawbacks, in **Table 2**. Moreover, the schematic designs of the newly developed spinneret configurations are represented in **Figure 3**.

4.1. Uniaxial Electrospinning or Electrospraying

The most common method of EHDP is uniaxial electrospinning or electrospraying, in which the spinneret is formed by one needle that contains a single fluid that is used to produce the polymer micro- and nanostructures. Despite its simplicity, different types of structures can still be developed using this classical method. Typically, a polymer is used, producing single micro- or nanostructures. However, by using more complex solutions, different polymer-based structures can be obtained. For instance, ultrathin polymer structures encapsulating lipophilic compounds can be developed using emulsions,[59] while using a dispersion of micro- or nanoparticles allows to produce composite micro- or nanofibers embedded in the polymer structures.[60]

Furthermore, uniaxial electrospinning or electrospraying also allows to create polymer coatings with increased functionality compared to, for example, solvent casting techniques.[52,53] In this regard, the electrospinning and electrospraying processes can also be combined in a sequential procedure to develop hierarchical structures based on functional coatings or surfaces with improved properties or multilayers with enhanced barrier or active performance. For instance, the deposition of silica (SiO_2)

Table 2. Different spinneret configurations for EHDP.

Configuration/method	Operating mode	Advantages	Drawbacks	Ref.
Uniaxial electrospinning or electrospraying	The spinneret is formed by a single needle and a single polymer solution is used to obtain polymer micro- or nanoparticles and/or micro- or nanofibers.	Straightforward and most used method. Versatile due to it can be adapted for different types of solutions, such as emulsions, and different modes of curation. It can be used to produce more uniform coatings, when compared with other techniques (e.g., solvent casting).	For polymer blends, electrospraying or electrospinning needs homogenization and leads to direct exposure to solvents. Unable to encapsulate water-soluble components in hydrophobic polymers and vice-versa. Distribution and release of drugs encapsulated in the polymers are poorly controlled.	[49–59]
Multiaxial electrospinning or electrospraying	The spinneret is formed by inserting needles of variable diameter inside larger needles, either in a concentric fashion or conventional one.	It produces more complex particles or fibers (e.g., hollow, core-shell, multi-layered, etc.). Encapsulated compounds are better protected from external conditions. More controllable release of encapsulated compounds. It can be modified to increase spraying or spinning times and yields (e.g., electroblowing).	It can be more difficult to optimize due to different ratios between polymers and compounds, compatibility between all polymers and solvents, and distance between the spinnerets. These parameters must be carefully considered.	[63–66]
Compound-fluidic electrospraying or multifluidic electrospinning	The spinneret is formed by grouping needles of variable diameters inside one larger needle. Internal needles can follow several configurations.	Allows the production of micro- or nanoparticles and/or micro- and nanofibers with multiple compartments in a single step. Compartments are separated through walls made from shell materials and different contents can be independently loaded. It allows better control and distribution of active and bioactive compounds.	Similar drawbacks than the multi-axial electrospraying, but at a lesser scale due to fewer needs for compatibility between polymer solutions and solvents are required. Special attention needs to be placed on the compatibility between the external and internal polymers and solvents.	[67–70]
Gas-assisted electrospinning and electrospraying	Several spinnerets can be used in this mode, with a key change being the addition of a flow of artificial gas pressure to the spinneret.	Makes use of artificial gas pressure in order to increase process productivity. Several configurations can be used to further increase productivity (e.g., including a gyrating spinneret).	It can require a high investment and a more complex design to control properly the product morphology. New parameters should be managed such as working pressure, infusion rate, rotational speed, and vessel and orifices geometry and size.	[71–73]
Side-by-side electrospinning or electrospraying	The spinneret is formed by placing needles on a side-by-side configuration.	It produces particles that will have the intrinsic properties of both polymers simultaneously. Allows to produce Janus particles in a straightforward and one-step process.	Difficulties in the reproducibility of the particle or fiber morphology and uniformity. Parallel flows may need to be optimized for optimal micro- or nanoparticle and/or micro- or nanofiber production.	[74–79]
Conjugate electrospinning or electrospraying	Two electrospinning or electrospraying heads are oppositely placed and charged with the collector centered between (above or below) them.	It allows the production of well-aligned fibers due to opposite charges. Improves solvent compatibility drawbacks in the use of side-by-side electrospraying or electrospinning to produce Janus particles or fibers. Allows more control over morphology and structure of Janus fiber or particles.	It shows higher costs of production due to the use of two electrospraying or electrospinning equipments. It associates increased polydispersibility of the produced particles and fibers. If the opposed jets are not both well-aligned, continuous particle and fiber formation will not be optimal (e.g., crossed fibers instead of parallel fibers).	[80–83]

(*Continued*)

Table 2. (Continued).

Configuration/method	Operating mode	Advantages	Drawbacks	Ref.
Simultaneous electrospinning/ electrospraying	One electrospinning head and one electrospraying head are used simultaneously, either with the same charge or opposing charges.	It allows for the development of patterned fibers with high functionalization. It produces complex structures in a one-step process without the need for additional chemical or mechanical treatments.	In addition to the optimization of both the electrospinning and electrospraying processes individually, optimization of the process/setup of deposition of the micro- or nanoparticles on the electrospun micro- or nanofibers is needed.	[84–86]
Electro-netting	It makes use of a typical electrospinning setup, using high voltages in order to produce 2D structures.	It allows producing both 2D and 3D structures in a simple, direct, and one-step process, with more strength and stability than fibers prepared by typical electrospinning techniques.	This process lacks productivity and stability. Currently formed nanowebs can be an intermittent result from a typical electrospinning process, severely affecting productivity.	[87,88]
Electrohydrodynamic jet printing	A mix of inkjet printing and electrospinning, where low voltages and tip-to-collector distance are used. The spinneret is formed by a solid probe.	It allows for a controlled deposition of fibers or particles through the decrease in the tip-to-collector distance, the use of low voltage, and a solid probe as the spinneret. More adequate for applications where pattern printing is a necessity.	For a proper visualization and high precision deposition of the micro- or nanofibers in the expected pattern, the use of a microscope is advised. Limitations exist regarding the use of more complex materials (e.g., functional and/or composite materials) and the production of more complex structures (e.g., layer-by-layer, hollow structures, etc.).	[89–92]
Multi-needle electrospinning and electrospraying	The spinneret is formed by grouping together several needles fed through individual or common syringes. Different groupings of needles can be used.	It allows an increase in production rate of micro- or nanoparticles due to the presence of more needle spinnerets and, therefore, more spraying cones.	More complex design, involving the placement of multiple needles. Question marks regarding uniformity. An adequate distribution of the electric field is also required for each needle to ensure proper distribution of jets.	[93–95]
Needle-less electrospinning and electrospraying	The spinneret can be formed by several geometries (e.g., a spinneret formed by a metallic plaque with an array of drilled holes, fed by a reservoir).	It allows an increase in the production yield when compared to typical electrospraying processes, similar to the multi-needle mode. It can be more cost-effective as no needles are needed to form the spinneret. It shows high versatility due to the possibility of using different collectors and spinnerets.	Plaque and reservoir need to have specific characteristics (e.g., hydrophobicity and dielectric properties). It is based on a complex design that requires optimization in the spatial arrangement of the array of holes and distance to the collector. Depending on the application, the collector should be changed.	[96–99]
Centrifugal electrospinning	The spinneret is formed by a rotating reservoir (either with an array of holes or needles) where the polymer solutions are held, surrounded by grounded collectors.	It allows to improve some of the drawbacks of typical electrospinning, such as low production rate and high-voltage requirements. A high production rate at low voltage can be achieved, but with low fiber alignment. High-fiber alignment is possible at high voltages.	The production of more complex (e.g., hollow fibers, multilayered structures, multiple compartments, etc.) is limited due to a single medium hosting reservoir is typically required. Production of highly aligned fibers is only possible at high voltages.	[37,100,101]

(*Continued*)

Table 2. (Continued).

Configuration/method	Operating mode	Advantages	Drawbacks	Ref.
Multi-pin electrospinning	The spinneret is formed by a combination of needle and needle-less electrospinning, using an array of half-sphere-shaped profiled pins.	The use of a pin setup, instead of the typical needle setup, improves needle clogging, particle settling, and uneven Taylor cone formation. Compared with needle-less electrospinning, lower voltages are needed.	It is based on a more complex spinneret design, leading to a need for optimization of both the pin profile and the spatial optimization of its distribution. Continuous production is hampered by the need to load the polymer solution to the pin surface.	[102]
Melt electrospinning	Temperature and a plasticizing system are used to melt the polymer, instead of using a solution.	Does not require the use of a solvent. It can be considered as a safer and green method to produce micro- or nanofibers than solution electrospinning when toxic solvents are involved. No residual solvent remains on the fibers and non-porous fibers are obtained. It can be used in a variety of operation methods (e.g., melt centrifugal, melt multi-needle, or needle-less electrospinning).	Limited applications due to the use of high temperature (e.g., encapsulation of thermolabile compounds) required to melt the polymers and the viscosity of the melted polymers. Limited structures can be produced compared to typical electrospinning processes. Higher voltages are required.	[103–106]

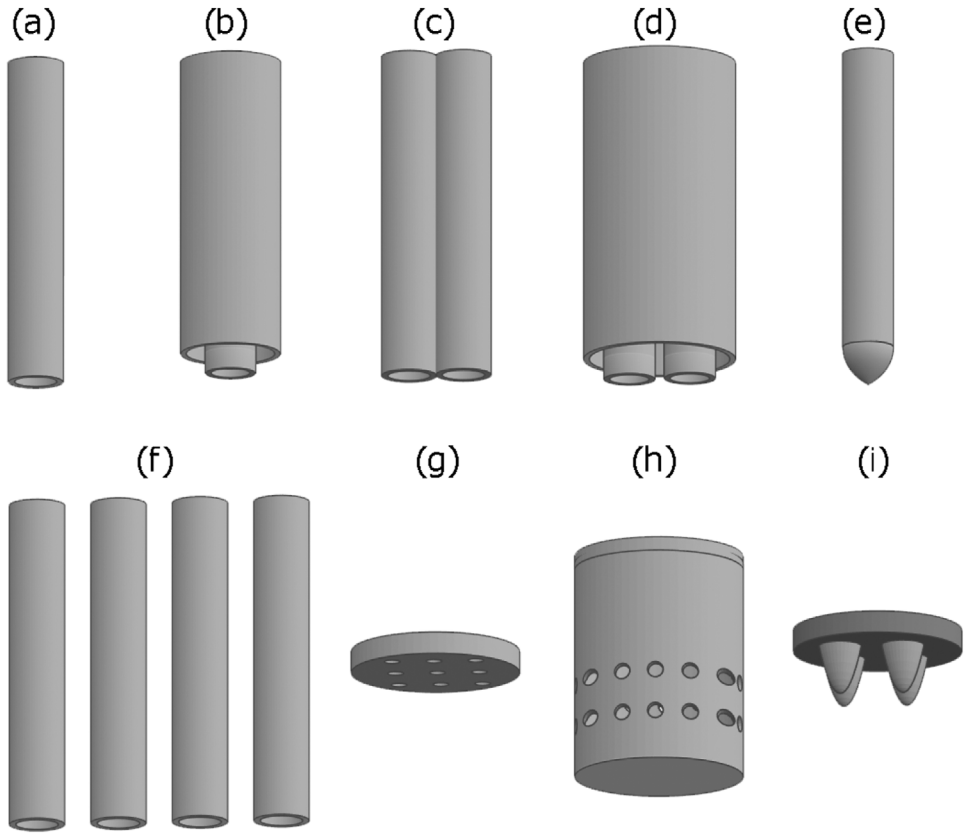

Figure 3. Schematic illustration of some of the different spinneret configurations available for EHDP: a) uniaxial; b) coaxial; c) side-by-side; d) multi-fluidic; e) electrohydrodynamic jet printing; f) multi-needle; g) needle-less; h) centrifugal; i) multi-pin.

microparticles on commercial plastic films, previously coated with electrospun polyester nanofibers, have yielded permanent and thermally stable superhydrophobic materials that can be used for food packaging and display easy-emptying properties for high-water activity goods.[61,62] Similarly, fully compostable multilayer structures with high-oxygen-barrier properties can be developed by incorporating electrospun mats of biodegradable polyesters and carbohydrates, followed by the application of a thermal post-treatment to promote layer adhesion.[54–56] Moreover, this methodology has successfully yielded multilayer systems with active and bioactive properties of interest in, for instance, antimicrobial packaging.[54,57,58]

4.2. Multiaxial Electrospinning or Electrospraying

Multiaxial electrospinning or electrospraying makes use of the same principle of the uniaxial method, but introducing needles with smaller diameters inside larger ones and also in different fashions. Multiaxial inserts one needle inside a larger one to setup its spinneret, while multifluidic spinnerets allow for the use of two or more needles inside a larger one. Both methods produce more complex structures, which can successfully allow increasing the functionality of the resultant polymer structures (e.g., better protection of the encapsulated compounds from solvents and ambient, a more controllable and sustained release of such compounds, etc.). In its simplest form, the coaxial spinneret is built up by inserting a small needle inside a larger one. The resulting core/shell structure, which comprises two different polymers with an inner/outer spatial relationship, represents the most frequently used configuration to produce functional nanomaterials. Nevertheless, more optimization in terms of processing parameters and designs is habitually needed when compared to uniaxial electrospinning due to solvent and polymer miscibility issues and the spatial configuration of the spinneret itself.[63,64]

In this regard, Yu et al.[63] successfully developed core/shell nanoparticles with a very thin outer layer that allowed a rapid dissolution of a poorly water-soluble drug (helicid). Therefore, using a modified coaxial electrospraying technique, the dissolution time of helicid increased up to two orders of magnitude when compared with the pure helicid. In another study, Huang et al.[65] made use of the coaxial electrospraying technique for the enhancement of the survival of probiotics in simulated gastrointestinal (GI) conditions. In this configuration, fish oil was incorporated into the core layer, together with sodium alginate and the probiotics, which was protected by an external shell layer that was composed by sodium alginate and pectin and by an outermost layer of soybean protein isolate. Survival of probiotics in the GI system was up to 94%, illustrating the potential of coaxial electrospinning for application in probiotic encapsulation in the food industry. In the field of coaxial electrospinning, it is remarkable the work performed by Abdelhakim et al.,[66] who developed core-sheath structures with the aim of masking the taste of a formulation of chlorpheniramine maleate for paediatric administration. Eudragit E PO and Kollicoat Smartseal were used to create layered nanofibers, alternating the polymers between the core and the shell of the system, as to identify the optimum taste-masked formulation, while the chlorpheniramine maleate was always loaded in the core. The best formulation, regarding the most effective taste-masking ability, contained Kollicoat Smartseal in the core with the chlorpheniramine maleate, and Eudragit E PO in the shell. An Insent E-tongue was used to determine the bitterness of the nano-sized fibers formulations and compare it with the pure chlorpheniramine maleate, confirming a successful taste masking since the bitterness of optimal formulation was undetected.

4.3. Compound-Fluidic or Multifluidic Electrospraying and Electrospinning

In the compound-fluidic or multifluidic configuration, the spinneret is formed by grouping needles of variable diameter, which can follow several configurations, inside a larger needle. For instance, Chen et al.[68] reported an experimental setup of multifluidic electrospraying that consisted of two metal capillaries that were inserted into a blunt metal needle to build a compound nozzle and were assembled individually from each other. As shown in **Figure 4**, different core fluids can be respectively fed to the metal capillaries at suitable flow-rates using this spinneret configuration, while a viscous shell fluid can be controlled and pumped out from the outer needle. Using this new setup, authors developed PVP/titanium composite microcapsules with multiple individual compartments that were able to be loaded independently, in a single step process. In particular, Somos 14120, glycerol, and paraffin oil were used directly as jetting liquids. Compartments were successfully separated from one another using shell materials, allowing for delivery of multiple compounds, where each of them can be individually loaded thus disregarding their possible interactions. According to the authors, this approach can potentially generate diverse microcapsules that could in one-step integrate different active components in a microscopic domain and free-of-contact manner, which may find potential applications in multicomponent drug delivery and microreactors, among others.

Other authors have also made use of the multifluidic configuration. For instance, Li et al.[69] used multifluidic electrospinning to develop colorimetric sensor strips for the detection of lead (II) ions (Pb^{2+}) using nanogold probes incorporated and immobilized onto polyamide 6 (PA6)/nitrocellulose (NC) nanofibers. Due to a significant increase in the specific surface area of the nanofibers, the stability of the gold nanoprobes was drastically increased, which allowed to reach a detection limit as low as 0.2 μM of Pb^{2+}. This value was able to induce the sensor color change from deep pink to white. The sensors were also tested in contact with other metal ions and only Pb^{2+} induced the pink to white color change, indicating the high selectivity of the developed colorimetric sensor strips. In another study, Zhang et al.[70] developed adsorption membranes for the removal of dyes in water purification processes using multi-fluidic electrospinning to produce polyethylene oxide (PEO) containing titanium dioxide and silicon dioxide (TiO_2-SiO_2) nanofibers of various morphologies. The resultant complex morphologies, namely mesoporous, hollow, or multichannel, showed enhanced properties such as high flexibility and large surface area (500 $m^2\ g^{-1}$), making these nanofibers extremely appropriate for dye adsorption (e.g., methyl blue). Furthermore, the newly produced mats displayed a high re-

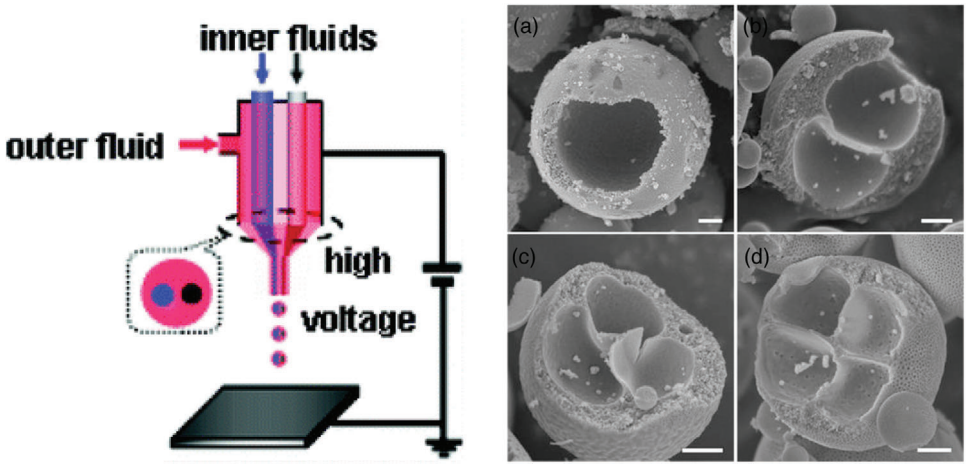

Figure 4. Experimental setup of compound-fluidic electrospraying (left) for the fabrication of microcapsules with several compartments (right). Reproduced with permission.[68] Copyright 2008, American Chemical Society.

sistance to adsorption-desorption cycles, indicating excellent recyclability properties.

4.4. Gas-Assisted Electrospinning and Electrospraying

One of the main disadvantages of the electrospinning and electrospraying processes is related to their low productivity, since these methods show processing throughputs that range, per single emitter, from some microliters to a few milliliters per h. In this regard, it has been recently demonstrated that fiber production can be effectively increased using artificial gas pressure. This approach is inspired by the principles of pressurized gyration (PG), which effectively combines high-speed rotation and gas pressure to extrude solution jets parallelly out from orifices that are located on the vessel surface.[73,107,108] PG is a voltage-free technology, originally established in 2013, that combines the features of solution blowing and centrifugal spinning to produce large quantities of homogenous fibers.[109] It is accomplished by connecting a pumped liquid infusion to a rotational vessel with holes, where the morphologies of the polymer structures can be customized by changing the features of vessel and orifices (geometry and size) and a stationary metal mesh can be placed around the vessel for quick collecting of the fibers.[107] Not using an electrical field offers the advantages of increasing scalability and reducing safety concerns whereas it can also offer the possibility to develop core-sheath structures by using water soluble and insoluble polymers.[110] Nevertheless, it should also be taken into account that both viscosity instabilities and solvent removal can be a limiting factor. In this regard, Ahmed et al.[73] compared fiber production via classical electric-field (EHDP) and pressure-driven (PG) methodologies for application in drug delivery. Four polymers were analyzed, namely PVDF, PMMA, poly(*N*-isopropylacrylamide) (PNIPAm), and PVP, whereas Amphotericin B and itraconazole were encapsulated. The use of PG allowed for a higher fiber production rate, which can be advantageous for process scalability. However, when comparing drug release by in vitro dissolution studies, the fibers produced by PG displayed a quicker drug release (within 15 min) than the electrospun fibers. This can be advantageous for the majority of pharmaceutical applications, where a more controlled release rate is desired instead of a quick or burst drug release. The different drug release profiles achieved were related to fiber size variations between the two methodologies, dependent upon the polymer. In particular, EHDP produced smaller fiber diameters for PVP (3.13 µm versus 3.53 µm for pressurized gyration) and PNIPAm (3.00 µm versus 6.30 µm for pressurized gyration), while PG produced smaller fiber diameters for PVDF (1.58 µm versus 4.63 µm for EHDP) and PMMA (1.97 µm versus 5.57 µm for EHDP).

In this context, artificial gas pressure and high voltages have been recently combined, yielding the so-called gas-assisted electrospinning or electroblowing, due to the promising potential of using pressurized gas to improve the scalability of conventional electrospinning processes. As illustrated in **Figure 5**, Shirazi et al.[72] used the gas-assisted electrospinning technology for the development of styrene-acrylonitrile and high-impact PS (SAN4-HIPS) nanofiber mats for application in the wastewater treatment industry as a direct contact distillation membrane (DCDM). The newly developed DCDMs were excellent in the removal of contaminants, with a reduction of 100% in color, close to 99.28% of chemical oxygen demand (COD), and 97.93% of biological oxygen demand (BOD). Nevertheless, a flux decline of up to 43% was observed after 48 h of DCDM processing, mainly caused by the fouling of the membrane, which is a key parameter for the use of these membranes in the long-term performance.

Also, based on the combination of electrospraying and PG principles, Busolo et al.[71] recently employed electrospraying assisted by pressurized gas (EAPG) to produce zein free-flowing powder at a throughput of 10 mL min^{-1}. The novel pilot installation comprised an injection unit, a drying chamber, and a cyclonic collector. In this new EHDP setup, nitrogen was continuously bubbled into the polymer solution and a pneumatic injector used compressed air/gas that nebulized within a high electric field. This technology was applied to encapsulate a fish oil highly enriched with docosahexaenoic acid (DHA) in ultrathin zein capsules that were, thereafter, used to fortify reconstituted milk, successfully masking the fish aroma.

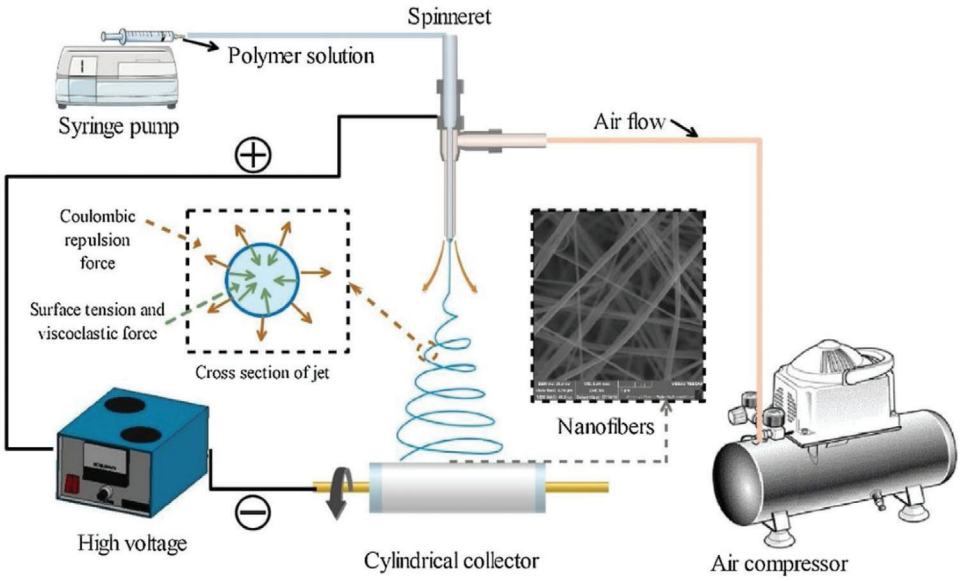

Figure 5. Schematic diagram illustrating gas-assisted electrospinning system equipment. Adapted with permission.[72] Copyright 2020, Elsevier.

4.5. Side-by-Side Electrospinning or Electrospraying

In this method, the spinneret is formed by placing needles on a side-by-side configuration. It can be used with one or multiple electrospinning or electrospraying heads and other configurations, allowing for the production of complex structures, such as Janus particles and fibers. It also simultaneously enables the final structure to have the intrinsic properties of all polymers used in its construction. In the side-by-side method, the spinnerets are aligned side-by-side, resulting in the merger of the nanostructures at the tip of the spinneret. Therefore, drawbacks regarding solvent and polymer solution miscibility's are avoided since the different solvents are never in contact with one another.

Side-by-side electrospinning has been particularly investigated to produce functional nanomaterials. Using this EHDP configuration, Sanchez-Vasquez et al.[76] were able to encapsulate a photosensitizer (rose bengal) and a cytotoxic drug (carmofur) in bicompartmentalized Janus particles of PVP, with a homogenous spherical morphology and a very low size distribution. The resultant Janus-structured particles, having two distinct faces with different properties, were highly selective for cancerous cells and proved the potential of side-by-side electrospraying to produce particles for photo-chemotherapy treatments. In another study, Yu et al.[77] presented a spinneret that was comprised of two acentric needles inside of a third metal needle to perform three-fluid electrospinning processes. This novel configuration was used to develop high quality PVP/shellac Janus nanofibers, utilizing an exterior solvent that surrounded the two core fluids arranged side-by-side, which was otherwise not feasible by uniaxial electrospinning. In another study, Seong-Min et al.[78] made use of side-by-side electrospinning to prepare PAN side-by-side nanofibers (SDS NFs) embedded with zinc oxide (ZnO) and silver nanoparticles (AgNPs), on opposite sides, thus forming a coupled fiber able that displays photo catalysis and antibacterial properties. These novel functional materials were applied in air filtration processes as membranes with enhanced organic contaminants' removal and antibacterial properties. Results showed a 97% dye degradation within 140 min of testing, while displaying antibacterial activity against Gram-positive (G+) and Gram-negative (G-) bacteria, versus 80% dye degradation for single nanofibers, also produced with ZnO and AgNPs, but with random orientation. In another research, Zhang et al.[79] used side-by-side electrospinning to produce polylactic acid (PLA) and poly(styrene-*co*-maleic anhydride) (PSMA) Janus fiber rods loaded with urease and folate that were aimed as self-propelled micromotors to improve tumor accumulation and cell internalization of therapeutic agents. The use of side-by-side electrospinning facilitated the production of Janus rid structures. The rod-like micromotors were able to promote tumor accumulation through the extension of the lateral drift in blood circulation, while the rod-like structure enhanced the leakage through the walls of the blood vessels.

Despite the advantages in the formation of new and complex structures in a facile one-step process, process optimization of side-by-side electrospinning is still complicated and continuous electrospinning or electrospraying is a requirement to ensure particle and fiber uniformity between the two polymers.[75–77] This side-by-side approach involves a complex interplay between fluid dynamics, electrodynamics, and rheology, and presents a challenge in controlling the movement in unison of two fluids under an electrical field between the spinneret and the collector.[76]

4.6. Conjugate Electrospinning or Electrospraying

In the conjugate electrospinning or electrospraying, the merger of structures occurs when the polymer solutions are in flight to the collector, which differs from side-by-side electrospinning. Thus, conjugate electrospinning or electrospraying is based on using two processing heads (twin-head), which are oppositely placed and charged, and a collector centered between (above or below) them.[80,81]

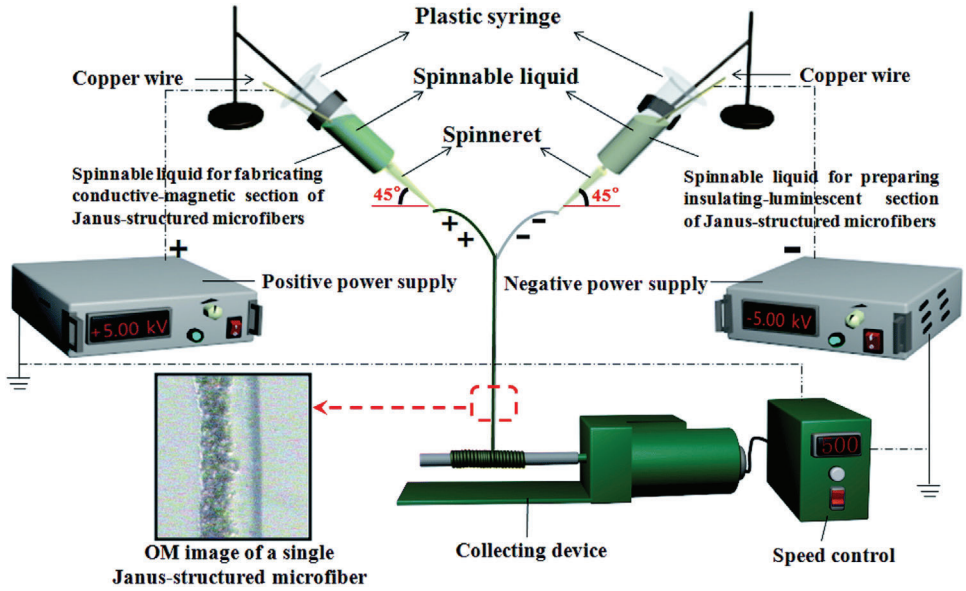

Figure 6. Schematic diagram of the conjugate electrospinning setup and spinning course. Reproduced with permission.[81] Copyright 2019, The Royal Society of Chemistry.

This novel EHDP method has also been very useful for the preparation of Janus-structured microfibers and capsules of interest in the development of -functional materials. In this regard, Mou et al.[80] prepared various Janus particles by means of oppositely charged twin-head electrospraying. In this setup, two TiO_2 precursor solutions were placed in separate syringes and then transferred via a tubing connection and syringe pumping to two separate metallic spray heads. A positive and a negative voltage were applied to the separate nozzles, which resulted in oppositely charged droplets that attracted and collided with each other. Following solvent evaporation and precursor gelation, the particles collided with each other and merged into one Janus particle due to Coulombic forces of attraction. In other research, Tian et al.[81] performed conjugate electrospinning to produce Janus-structured microfibers that comprised polyaniline (PANI)/magnetite (Fe_3O_4)/PMMA, as a conductive–magnetic segment, and rare-earth or europium complex [$Eu(TTA)_3(TPPO)_2$]/PMMA, as an insulating–luminescent segment. The particular setup used for the fabrication of this Janus structure is shown in **Figure 6**, which was based on two high-voltage DC power supplies outputting positive and negative voltages, respectively. The two spinnable liquids were added individually into plastic syringes, which were positioned in opposite directions, and both were positioned at an angle of ≈45° from the horizontal. Two pieces of copper wire were used as the electrodes, being separately plunged into the spinnable liquids. Finally, the collection device consisted of a rotating metal rod covered with aluminum foil.

The resulting functional materials prepared by conjugate electrospinning are very promising for biomedical applications. For instance, Kuang et al.[82] made use of conjugate electrospinning to produce heparin (HEP)/silk and poly(L-lactide-*co*-ε-caprolactone) P(LLA-*co*-CL) composite nanofibers that can be developed into small size artificial blood vessel implants. When tested in in vivo animal experiments, the produced grafts remained open for more than 8 months, while the regenerated vascular tissues (aided by the release of HEP) offered similar functionality as that of autogenous vascular tissue. As such, the use of conjugate electrospinning to produce composite nanofibers proved to be successful with a view of developing blood vessel grafts since these could maintain long-term patency in vivo while successfully remodeling the vascular tissue. In another study, Jin et al.[83] also made use of conjugate electrospinning for application in the biomedical industry. The authors produced nanofibers of P(LLA-*co*-CL), silk fibroin (SF), and PEO, loaded with HEP to develop an artificial mono-layered vascular scaffold, which was assessed in a rabbit model through the transplantation of an orthotopic rabbit carotid artery. In vivo remodeling was evaluated after three months and the transplantation and remodeling of the HEP/SF/PEO scaffold resulted in a regenerated smooth muscle layer that was coated by an uninterrupted endothelium.

4.7. Simultaneous Electrospinning/Electrospraying

Another novel EHDP method that makes use of multiple heads is simultaneous electrospinning/electrospraying. In this method, both ultrathin fibers and particles can be produced simultaneously. Particles are generally deposited on the surface of the fiber mats in a one-step process, creating complex and highly functional structures that can be applied in multiple fields, such as in the biomedical or electronics.[84,85] For instance, Korina et. al.[84] experimented a novel EHDP setup (see **Figure 7**) that was comprised of a stainless-steel coaxial spinneret, situated perpendicularly toward the collector. It consisted on an inner and an outer reservoirs connected to two syringe pumps for delivering the core and shell solutions simultaneously without mixing. In the same setup, another pump was used for delivering the electrospraying dispersion by means of an additional high voltage supply. Authors successfully developed

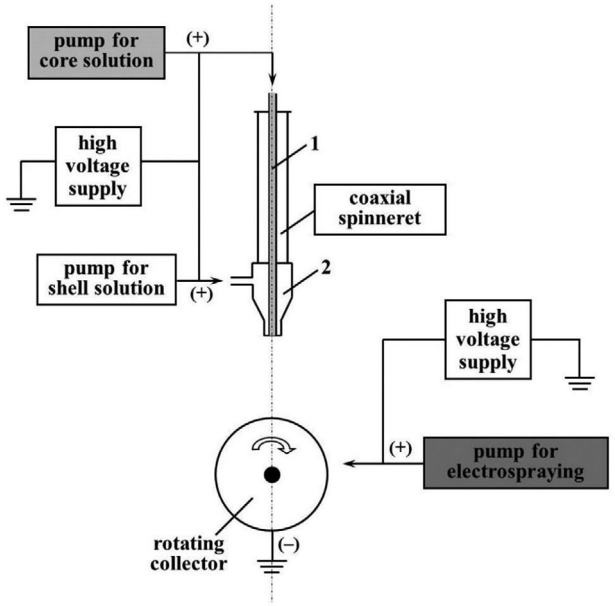

Figure 7. Schematic illustration of the experimental setup for simultaneous coaxial electrospinning and electrospraying with 1) inner and 2) outer reservoirs. Reproduced with permission.[84] Copyright 2018, Elsevier.

electrospun Fe_3O_4/PVA–poly(3-hydroxybutyrate) (PHB)/poly(ϵ-caprolactone) (PCL) core-shell fibers coated with an electrosprayed TiO_2/chitosan oligosaccharides (COS) dispersion, which can be promising for applications of water and air purification from organic pollutants. Following a similar setup, DeVolder et al.[85] created an angiogenic microfiber patch that allowed for the controlled release of angiogenic growth factors (vascular endothelial growth factor, VEGF) from PLA microfibers covered with VEGF-encapsulating poly(lactide-*co*-glycolide) (PLGA) microparticles. This patch, when implanted, was able to form new blood vessels with controlled spacing and directionality, an important step for clinical treatments that require neovascularization. In another research study, Spasova et al.[86] used simultaneous electrospinning and electrospraying for the development of sustainable nanomaterials with potential antifungal activity against *P. chlamydospore*, which causes esca, a grapevine trunk disease that reduces vine yield and longevity. The authors used biodegradable and biocompatible polymers, namely PHB, nanosized TiO_2-anatase (nanoTiO2), and COS. The use of simultaneous electrospinning and electrospraying techniques resulted in PHB fibers with nanoTiO_2 deposited on the fibers' surface, that is, TiO_2-*on*-PHB, which displayed complete fungal growth inhibition against *P. chlamydospore*, proving their suitability for application against esca in agriculture.

4.8. Electro-Netting and Electrohydrodynamic Jet Printing

In addition to the previously mentioned EHDP methods and spinneret modifications, other methods have also been developed to produce new structures, namely electro-netting and electrohydrodynamic jet printing. Electro-netting allows for the development of 2D structures in a one-step process by working in a state of instability resulting from the use of very high voltages to induce the formation of 2D networks of fibers during their flight to the collector. However, this process is still in its early stages and, therefore, advancements are still needed, particularly in the productivity of the 3D nanowebs and their process stability. In this regard, Zhang et al.[87] developed a method to create advanced self-assembled 2D nanofibrous networks based on PVDF and PAN. Through precise tailoring of precursors and electrical field, the ejected charged droplets levitated, deformed, and phase-separated before self-assembling in a 2D nanoarchitecture. Electro-netting can be effectively employed, for example, to produce 2D nanowebs that better mimic the behavior of the extracellular matrix (ECM) by using biocompatible polymers. Furthermore, Liu et al.[88] also used the electro-netting technique to produced 2D nanofiber networks, which consisted of nanofibers interlinked at a large scale. These 2D nanonets, produced from PAN, with a diameter of around 30 nm, showed a spider web-like network structure and a small pore size (≈0.26 µm). These functional materials were then used to develop an ultrathin (≈0.4 µm) and ultra-light (0.68 g m^{-2}) air filter. These characteristics, in combination with a high porosity (92.1%), allowed the filters to display an air resistance of 73.5 Pa, with an enhanced particulate matter capture capacity ($PM^{0.3}$ removal efficiency of 99.996%).

Electrohydrodynamic (EHD) jet printing, also called EHD jetting, follows a slightly more advanced performance than electronetting. It makes use of the classical setup of electrospinning, but the spinneret is usually changed from needles to solid probes, using a much lower tip-to-collector distance that allows a higher control deposition of fibers. This new arrangement allows creating printing patterns, especially useful for electronics and the development of sensors. Recent studies have demonstrated that it can be used in two different modes, namely continuous near-field electrospinning (NFES) and dot-based drop-on-demand (DOD) EHD printing.[89–91] For instance, George et al.[90] used NFES to develop a high-resolution nanopatterning method that produced aligned graphitized micro- and nanowires as precursors for high-throughput carbon nanomanufacturing. This work also demonstrated that the diameter and straightness of the nanowires can be controlled by adjusting the voltage and the tip-to-collector distance. In another research study, Liashenko et al.[91] presented a new experimental strategy, shown in **Figure 8**, based on the control of the trajectory of an electrified jet by means of rapidly tuning the surrounding electrostatic field through additional electrodes. This process enabled a fast-printing process in nozzle-based 3D printing techniques. As a result, 3D structures of PEO of various M_{Ws} containing AgNPs with increasing complexity, including crossovers and bridges, were printed by precise electrostatically driven layer-by-layer self-assembly at frequencies as high as 2000 layers per s through electrostatic deflection of electrified jets.

In this regard, it is also worth mentioning that Suihong et al.[92] used EHD jet printing as one of the processes for the development of gelatin-based biomimetic triple-layered conduits for nerve tissue engineering. The EHD jet printing was applied to produce the innermost layer using PCL, which comprises the most intricate structural details, and the outer layer of PCL. This intricate inner structure allowed for the enhancement of the mechanical strength of the conduits, while inducing directional growth along the aligned filaments, whereas the outer layer promoted cell adhesion. Analysis of the produced triple-layered con-

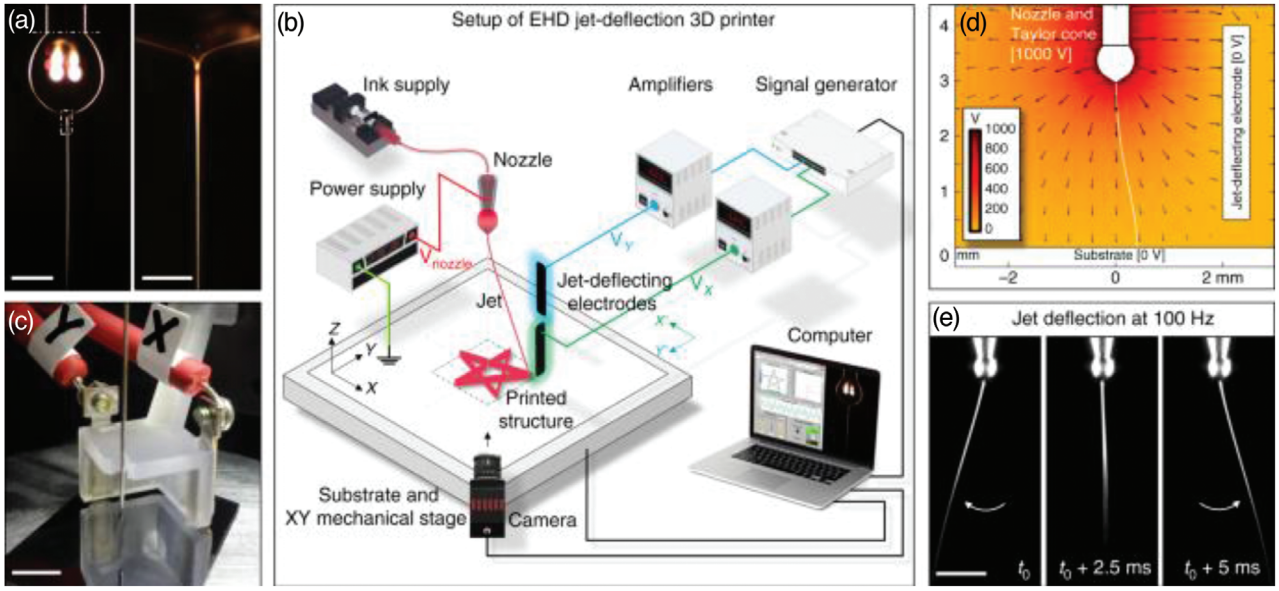

Figure 8. Electrohydrodynamic (EHD) jetting showing: a) Optical photographs of the nozzle, ink drop (below-dotted line), Taylor cone, and the electrified jet with scale bars of 500 and 50 µm; b) Schematic of an EHD 3D printer with jet-deflecting electrodes; c) Set of jet-deflecting electrodes and needle used as nozzle with a scale bar of 5 mm; d) Simulation of the electric potential and field around the jet in the presence of a jet-deflecting electrode; e) High-speed video captures of the jet being deflected in 1D with a frequency of 100 Hz with a scale bar of 500 µm. Reproduced with permission.[91] Copyright 2020, Springer Nature.

duits displayed appropriate mechanical properties for human sciatic nerve repair, while the porosity of the conduits facilitated cellular infiltration, neuronal precursor, as well as vascular cell growth.

4.9. Multi-needle and Needle-Less Electrospinning and Electrospraying

As stated previously, one of the major drawbacks of typical electrospinning and electrospraying processes is the low production yield of the micro- and nanostructures. Thus, multi-needle electrospinning or electrospraying has also been proposed as one of the alternatives to improve productivity. In the multi-needle configuration, multiple needles are used in order to increase the number of Taylor cones and, thus, increase the productivity of the process. As an alternative to multi-needle electrospinning or electrospraying, needle-less (or free surface) electrospinning or electrospraying has also been developed. A variety of non-needle spinnerets can be used, as displayed in **Figure 9** (e.g., wire, cylinders, discs, among others) but, due to process limitations, significantly higher voltages are typically needed. In particular, the use of a needle spinneret makes it easier to form a droplet shape that is easily turned into a Taylor cone through applied voltage.[93,94,96,97] For example, Parhizkar et al.[93] optimized a multi-needle electrospraying system in order to increase the inherently low productivity of uniaxial electrospinning. Two different spinnerets were tested (four needles in a circular and linear distribution) and it was demonstrated that cone jets were more stable for the circular spinneret distribution, obtaining a lower size distribution and requiring the use of less voltage than the linear one. Both configurations had similar production yields, resulting approximately 4 times higher than with a single needle.

In relation to the needle-less electrospinning technique, Ryšánek et al.[97] were able to develop hollow nanofibers using a wire electrode as the spinneret. The formation of hollow fibers was attributed to the choice of PAN as the polymer, displaying both the potential to produce different nanostructures by needle-less electrospinning and the influence of the polymeric chain and crystal structure on the final morphology of nanostructures. In another study, Yu et al.[98] used a multi-needle electrospinning technique for the production of fibers of polyethyleneimine (PEI) containing graphene oxide (GO) that were able to load Ag-NPs as an antibacterial agent. The antibacterial activity of the developed fabric was assayed and reported reduction values as high as 99.99% for both *Escherichia coli* and *Staphylococcus aureus*, even after 10 washes, demonstrating exceptional stability. As a result, the produced nanofiber yarn shows a great deal of potential for the development and production of antibacterial textiles. Wei et al.[99] also used a needless electrospinning technique for the production of tin(IV) oxide (SnO_2)/TiO_2 side-by-side bi-component nanofibers (SBNFs), composed by a V-channel needle-less spinneret. The produced SNBFs were dissymmetric and were formed by a small SnO_2 nanofiber (20–80 nm) and a larger, Sn-doped, TiO_2 nanofiber (≈250 nm). These nanofibers were used to develop dye-sensitized solar cells (DSSCs) that displayed a maximum power conversion efficiency (PCE) of 8.3%, being 2.6-fold higher than DSSCs based on standalone TiO_2 nanofibers, demonstrating the potential of these functional nanofibers for high-performance photoelectrochemical devices.

4.10. Centrifugal and Multi-Pin Electrospinning

In an effort to combine the advantages of regular electrospinning, multi-needle, and needle-less electrospinning, other novel

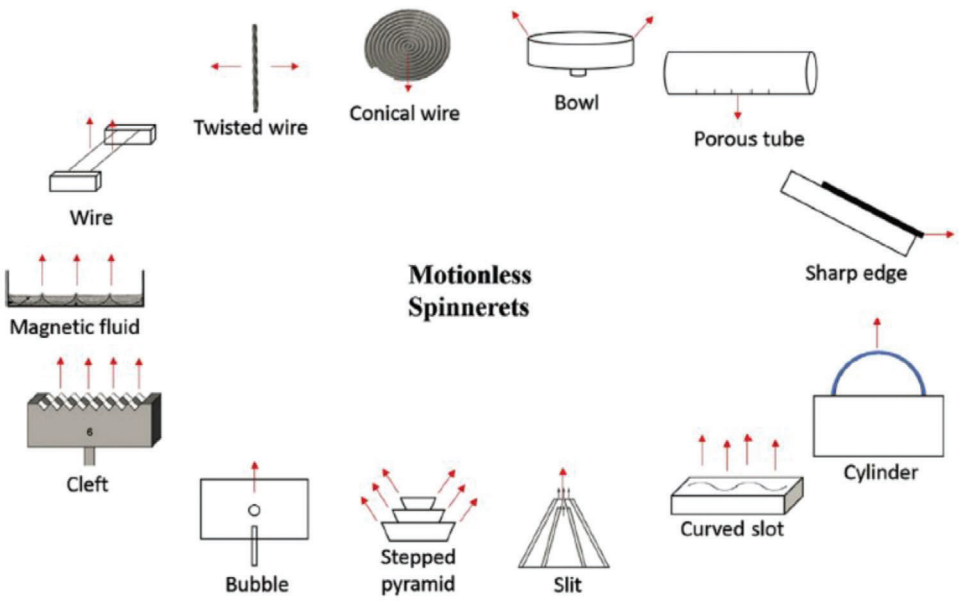

Figure 9. Schematic representation of several needle-less spinnerets. Reproduced with permission.[95] Copyright 2018, Elsevier.

and more intricate methods have been created. In this regard, centrifugal electrospinning makes use of both electrostatic and centrifugal forces in order to reduce the need for high voltages. The spinneret is constituted by a rotational reservoir with multiple needles (or with an array of holes), where the polymer solution is stored, and it is surrounded by the grounded collectors. Multi-pin electrospinning also tackles typical electrospinning technical issues and limitations (e.g., low production yield and clogging), making use of solid half-sphere-shaped profiled pins instead of needles. As a result, it provides advantages regarding clogging and, due to its particular profile, shaped pins facilitates the formation and stabilization of the Taylor cones.[37,100,102]

In this context, Chang et al.[100] developed ultrathin nanofibers of PAN/PMMA using centrifugal electrospinning with a multi-needle reservoir rotating at 4000 rpm. The electrospun fibers had a diameter remarkably lower than those formed by typical electrospinning due to the influence of centrifugal force on the stretching of fibers, leading to ultrathin fibers that displayed better electrochemical properties. In another research, Prabu and Dhurai[102] developed a novel profiled multi-pin electrospinning (PMES) to solve some drawbacks of other electrospinning techniques. As an example of this, **Figure 10** shows the PMES setup used for PVA nanofiber production encapsulating zinc oxide nanoparticles (ZnONPs). The setup consisted of a high-voltage voltage source, a polymer tank, a profiled multi-pin spinneret construction. In this arrangement, sphere-shaped polymer jets and Taylor cones were formed, while fibers were collected in a grounded flat metal collector. The up and down motion was controlled through an electrical timer circuit and the timing was fixed at 15 and 2 s for upward and downward movement, respectively. Both the profiled pin arrangement and the use of solid probes aided in the formation of Taylor cone, prevented problems such as needle clogging, and led to productivities similar to those of needle-less systems. In particular, this prototype design was composed of 21 pins of 25 mm length and 3.5 mm diameter, and it achieved the production of 1.780 g h^{-1}.

Furthermore, Huang et al.[101] also used a centrifugal electrospinning method to produce platinum nanowires for use as part of a proton exchange membrane fuel cell (PEMFC). The nanowires were produced from a polymer solution composed of PVP and hexachloroplatinic acid hydrate (Cl_6H_4OPt). The produced nanowires displayed a diameter of ≈54 nm and an electrochemically active surface area of 5.64 m^2 g^{-1}. Through accelerated degradation tests it was seen that the platinum nanowires displayed better durability than commercial platinum and carbon. Furthermore, the fuel cell performance in PEMFC was enhanced by combining the platinum nanowires with a platinum and carbon mixture.

4.11. Melt Electrospinning

One of the main advantages of electrospinning over other converting technologies dealing with polymer materials is that it does not require the use of high temperature, however, the use of a solvent is a requirement. Oppositely, melt electrospinning couples a plasticizing or melting (heating) system to the basic setup of electrospinning to promote the softening or melting of the polymers, in the case of thermoplastic materials, which then avoids the use of solvents. Furthermore, a higher throughput can be achieved due to the absence of loss in mass by solvent evaporation. Different spinnerets and configurations can also be used such as melt centrifugal differential electrospinning and needleless melt differential electrospinning, among others.[103,104] Indeed, as similar to classical solution electrospinning, melt electrospinning has also evolved into novel and complex designs. For instance, Nam and Park[105] produced PLA microbeads through melt electrospraying for the development of a sustainable alternative to currently used additives in the cosmetic industry. The au-

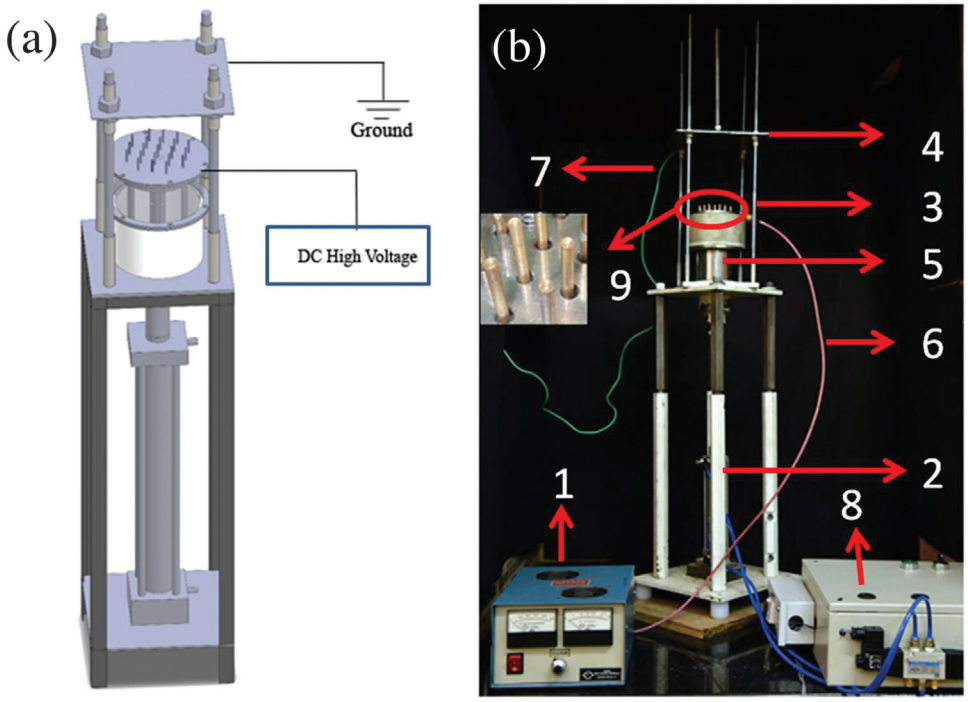

Figure 10. Profiled multi-pin electrospinning system (PMES) setup: a) Schematic diagram of PMES; b) Fabricated PMES setup showing 1) direct current (DC) high-voltage power source, 2) spinneret drive arrangement, 3) profiled multi-pin spinneret, 4) stationary flat collector, 5) polymer reservoir, 6) DC high-voltage cable, 7) grounding cable, 8) pneumatic circuit, and 9) profiled multi-pin magnified view. Reproduced with permission.[102] Copyright 2020, Springer Nature.

thors used electron beam (E-beam) irradiation to control the melt processability of PLA and were able to prepare biodegradable microbeads. Over time PLA microbeads showed bulk degradation, leading to decreasing residual weights, structural, and thermal stability. The produced microbeads also displayed a poor adsorption behavior of persistent organic pollutants (POPs) due to their low specific surface area that, combined with the green nature of the melt electrospinning method, highlights its potential to replace non-biodegradable microbeads in cosmetics. Buivydiene et al.[106] also made use of a combined method of solution and melt electrospinning for the production of polyamide 12 (PA12) fiber mats that can be potentially applied as fibrous air filters. Authors were able to develop submicron (<1 μm) and supermicron (≥1 μm) structured fibrous mats that presented favorable filtration properties, such as high-filtration quality (0.068–0.085 Pa^{-1} for PN_1 fraction), low values of pressure drops (15.92–50.17 Pa), and with high filtration efficiencies ranging from 94% (PN_1) to 99% (PN_{10}). The filtration quality factors were associated with the fiber size, in which higher quality ratios of filtration were attained by using fiber mats with higher sub-to-super micrometer ratios.

5. Concluding Remarks and Future Trends

EHDP shows promising potential for widespread adoption as functional materials in several industries, particularly in the food packaging, pharmaceutical, environmental, and biomedical industries as well as in the areas of energy and electronics. In particular, the combination of different materials with diverse properties and the wide range of modes of operation allow developing unique micro- and nanostructures with active properties (e.g., multi-layered, core-shell, Janus particles or fibers, among others). Moreover, the possibility of processing at room conditions is a key differential to other drying and encapsulation technologies. Since EHDP allows the processing of heat or pressure labile compounds, it will be an encouraging factor for its widespread adoption in applications related to biotechnology and biosensors.

Although EHDP is a straightforward and versatile method to fabricate polymer micro- and nanostructures, its operational parameters, that is, solvent type and solution properties, processing conditions, that is, flow-rate, voltage, tip-to-collector distance, etc., and room conditions, that is, temperature and relative humidity, can strongly affect the morphology and, hence, the final characteristics of the resultant materials. This turns out to be one of the main drawbacks of EHDP since such a high influence of the operational parameters results in each material needing its own optimization. However, the research studies performed during the last decade have demonstrated that optimization can be effectively conducted and the control of the EHDP parameters should not be viewed as a major concern. Other issues that might arise, especially when it comes to newly developed methods of operation, are the homogeneity of the end products as well as concerns over their relatively low throughput. Nevertheless, some novel operation methods have been developed recently in the EHDP area, such as assisted gas, multi-needle spinnerets, needless, or centrifugal electrospinning, allowing for an effective increase in productivity. Other novel techniques, such as electronetting and EHD jet printing, have successfully combined the advantages of EHDP with other novel techniques.

In any case, most of these new advances in the EHDP area are still in their early stage, thus they will need further development and research to ascertain their actual potential. Furthermore, the micro- and nanostructures attained by EHDP need to be carefully characterized and assessed, namely regarding their safety, particularly when aimed to be used in the biomedical, pharmaceutical, and food industries, including their cytotoxicity, digestibility, and bioavailability of encapsulated components.

Acknowledgements

This study was supported by the Portuguese Foundation for Science and Technology (FCT) under the scope of the strategic funding of UIDB/04469/2020 unit and by the I&D&I AgriFood XXI project, operation number NORTE-01-0145-FEDER-000041, co-financed by the European Regional Development Fund (FEDER) under the scope of NORTE 2020 (Programa Operacional Regional do Norte 2014/2020). Pedro Silva is the recipient of a fellowship (SFRD/BD/130247/2017) supported by FCT. S. Torres-Giner acknowledges Spanish Ministry of Science and Innovation (MICI) for the funding received during his Ramón y Cajal contract (RYC2019-027784-I).

Conflict of Interest

The authors declare no conflict of interest.

Keywords

electrohydrodynamic processing, high-throughput electrospinning, multicomponent materials, operational parameters, spinneret configuration

Received: November 15, 2021
Revised: January 7, 2022
Published online: February 4, 2022

[1] L. Rayleigh, *London, Edinburgh Dublin Philos. Mag. J. Sci.* **1882**, *14*, 184.
[2] J. Zeleny, *Phys. Rev.* **1914**, *3*, 69.
[3] J. Zeleny, *Phys. Rev.* **1917**, *10*, 1.
[4] A. Formhals, US1975594, **1934**.
[5] A. Formhals, US2160962, **1939**.
[6] A. Formhals, US2187306A, **1940**.
[7] A. Formhals, US2323025, **1943**.
[8] B. Vonnegut, R. L. Neubauer, *J. Colloid Sci.* **1952**, *7*, 616.
[9] G. Taylor, *Proc. R. Soc. London, Ser. A* **1964**, *280*, 383.
[10] G. Taylor, *Proc. R. Soc. London, Ser. A* **1969**, *313*, 453.
[11] T. Senthil Muthu Kumar, K. Senthil Kumar, N. Rajini, S. Siengchin, N. Ayrilmis, A. Varada Rajulu, *Composites, Part B* **2019**, *175*, 107074.
[12] P. J. García-Moreno, A. C. Mendes, C. Jacobsen, I. S. Chronakis, in *Polymers for Food Applications*, Springer, New York **2018**, pp. 447–479.
[13] L. Deng, X. Kang, Y. Liu, F. Feng, H. Zhang, *Food Hydrocolloids* **2018**, *74*, 324.
[14] Y. Liao, C.-H. Loh, M. Tian, R. Wang, A. G. Fane, *Prog. Polym. Sci.* **2018**, *77*, 69.
[15] R. M. Rodrigues, P. E. Ramos, M. F. Cerqueira, J. A. Teixeira, A. A. Vicente, L. M. Pastrana, R. N. Pereira, M. A. Cerqueira, *Food Chem.* **2020**, *314*, 126157.
[16] L. Li, S. Peng, J. K. Y. Lee, D. Ji, M. Srinivasan, S. Ramakrishna, *Nano Energy* **2017**, *39*, 111.
[17] A. W. Jatoi, H. Ogasawara, I. S. Kim, Q.-Q. Ni, *Mater. Sci. Eng., C* **2020**, *110*, 110679.
[18] A. Haider, S. Haider, I.-K. Kang, *Arabian J. Chem.* **2018**, *11*, 1165.
[19] V. D. F. Martins, M. A. Cerqueira, P. Fuciños, A. Garrido-Maestu, J. M. R. Curto, L. M. Pastrana, *Cellulose* **2018**, *25*, 6361.
[20] M. J. Costa, L. M. Pastrana, J. A. Teixeira, S. M. Sillankorva, M. A. Cerqueira, *Innovative Food Sci. Emerging Technol.* **2021**, *69*, 102646.
[21] S. R. Jang, J. I. Kim, C. H. Park, C. S. Kim, *Mater. Sci. Eng., C* **2020**, *111*, 110776.
[22] G. Paimard, M. Shahlaei, P. Moradipour, H. Akbari, M. Jafari, E. Arkan, *Sens. Actuators, B* **2020**, *311*, 127928.
[23] W. Guo, C. Tan, K. Shi, J. Li, X.-X. Wang, B. Sun, X. Huang, Y.-Z. Long, P. Jiang, *Nanoscale* **2018**, *10*, 17751.
[24] X. Wang, C. Drew, S.-H. Lee, K. J. Senecal, J. Kumar, L. A. Samuelson, *Nano Lett.* **2002**, *2*, 1273.
[25] A. M. Marques, M. A. Azevedo, J. A. Teixeira, L. M. Pastrana, C. Gonçalves, M. A. Cerqueira, in *Food Applications of Nanotechnology*, CRC Press, Boca Raton, FL **2019**, pp. 61–97.
[26] P. M. Silva, C. Prieto, J. M. Lagarón, L. M. Pastrana, M. A. Coimbra, A. A. Vicente, M. A. Cerqueira, *Food Hydrocolloids* **2021**, *118*, 106761.
[27] V. R. Rai, J. A. Bai, M. J. Costa, P. E. Ramos, P. Fuciños, J. A. Teixeira, L. M. Pastrana, M. Â. Cerqueira, in *Nanotechnology Applications in the Food Industry*, CRC Press, Boca Raton, FL **2019**, pp. 3–20.
[28] J. Wang, J. A. Jansen, F. Yang, *Front. Chem.* **2019**, http://doi.org/10.3389/fchem.2019.00258.
[29] P. M. Silva, S. Torres-Giner, A. A. Vicente, M. A. Cerqueira, *Curr. Opin. Colloid Interface Sci.* **2021**, *56*, 101504.
[30] F. Zhang, Q. Ni, O. Jacobson, S. Cheng, A. Liao, Z. Wang, Z. He, G. Yu, J. Song, Y. Ma, G. Niu, L. Zhang, G. Zhu, X. Chen, *Angew. Chem., Int. Ed.* **2018**, *57*, 7066.
[31] J. Fernández De La Mora, *Annu. Rev. Fluid Mech.* **2007**, *39*, 217.
[32] A. M. Gañán-Calvo, J. M. López-Herrera, M. A. Herrada, A. Ramos, J. M. Montanero, *J. Aerosol Sci.* **2018**, *125*, 32.
[33] M. Cloupeau, B. Prunet-Foch, *J. Electrost.* **1990**, *25*, 165.
[34] M. Cloupeau, B. Prunet-Foch, *J. Aerosol Sci.* **1994**, *25*, 1021.
[35] H. Zong, X. Xia, Y. Liang, S. Dai, A. Alsaedi, T. Hayat, F. Kong, J. H. Pan, *Mater. Sci. Eng., C* **2018**, *92*, 1075.
[36] A. Alehosseini, B. Ghorani, M. Sarabi-Jamab, N. Tucker, *Crit. Rev. Food Sci. Nutr.* **2018**, *58*, 2346.
[37] H. S. Salehhudin, E. N. Mohamad, W. N. L. Mahadi, A. Muhammad Afifi, *Mater. Manuf. Processes* **2018**, *33*, 479.
[38] S. L. Shenoy, W. D. Bates, H. L. Frisch, G. E. Wnek, *Polymer* **2005**, *46*, 3372.
[39] M. G. Mckee, G. L. Wilkes, R. H. Colby, T. E. Long, *Macromolecules* **2004**, *37*, 1760.
[40] D. M. Correia, R. Gonçalves, C. Ribeiro, V. Sencadas, G. Botelho, J. L. G. Ribelles, S. Lanceros-Méndez, *RSC Adv.* **2014**, *4*, 33013.
[41] A. Smeets, C. Clasen, G. Van Den Mooter, *Eur. J. Pharm. Biopharm.* **2017**, *119*, 114.
[42] S. Zhang, C. Campagne, F. Salaün, *Appl. Sci.* **2019**, *9*, 402.
[43] F. Topuz, B. Satilmis, T. Uyar, *Polymer* **2019**, *178*, 121610.
[44] W. Fang, S. Yang, T.-Q. Yuan, A. Charlton, R.-C. Sun, *Ind. Eng. Chem. Res.* **2017**, *56*, 9551.
[45] G. Yazgan, A. M. Popa, R. M. Rossi, K. Maniura-Weber, J. Puigmartí-Luis, D. Crespy, G. Fortunato, *Polymer* **2015**, *66*, 268.
[46] H. Zhou, Z. Shi, X. Wan, H. Fang, D.-G. Yu, X. Chen, P. Liu, *Nanomaterials* **2019**, *9*, 843.
[47] E. Jain, K. M. Scott, S. P. Zustiak, S. A. Sell, *Macromol. Mater. Eng.* **2015**, *300*, 823.
[48] J. Pelipenko, J. Kristl, B. Janković, S. Baumgartner, P. Kocbek, *Int. J. Pharm.* **2013**, *456*, 125.
[49] X. Huang, J. Gao, N. Zheng, W. Li, H. Xue, R. K. Y. Li, *Colloids Surf., A* **2017**, *517*, 17.
[50] X.-X. Wang, X.-J. Ju, S.-X. Sun, R. Xie, W. Wang, Z. Liu, L.-Y. Chu, *RSC Adv.* **2015**, *5*, 34243.

[51] G.-Z. Yang, H.-P. Li, J.-H. Yang, J. Wan, D.-G. Yu, *Nanoscale Res. Lett.* **2017**, *12*, 55.
[52] A. Javadi, A. Solouk, M. Haghbin Nazarpak, F. Bagheri, *Mater. Sci. Eng., C* **2019**, *99*, 620.
[53] H. Wang, W. Li, Z. Li, *Nanoscale* **2018**, *10*, 18857.
[54] K. Figueroa-Lopez, S. Torres-Giner, I. Angulo, M. Pardo-Figuerez, J. Escuin, A. Bourbon, L. Cabedo, Y. Nevo, M. Cerqueira, J. Lagaron, *Nanomater.* **2020**, *10*, 2356.
[55] B. Melendez-Rodriguez, S. Torres-Giner, I. Angulo, M. Pardo-Figuerez, L. Hilliou, J. M. Escuin, L. Cabedo, Y. Nevo, C. Prieto, J. M. Lagaron, *Nanomaterials* **2021**, *11*, 1443.
[56] B. Akinalan Balik, S. Argin, J. M. Lagaron, S. Torres-Giner, *Appl. Sci.* **2019**, *9*, 5136.
[57] K. J. Figueroa-Lopez, L. Cabedo, J. M. Lagaron, S. Torres-Giner, *Front. Nutr.* **2020**, *7*, 140.
[58] L. Quiles-Carrillo, N. Montanes, J. Lagaron, R. Balart, S. Torres-Giner, *Appl. Sci.* **2019**, *9*, 533.
[59] J. Hu, M. P. Prabhakaran, X. Ding, S. Ramakrishna, *J. Biomater. Sci., Polym. Ed.* **2015**, *26*, 57.
[60] S. Torres-Giner, A. Martinez-Abad, J. M. Lagaron, *J. Appl. Polym. Sci.* **2014**, *131*, n/a.
[61] M. Pardo-Figuerez, A. López-Córdoba, S. Torres-Giner, J. M. Lagaron, *Coatings* **2018**, *8*, 364.
[62] J. Lasprilla-Botero, S. Torres-Giner, M. Pardo-Figuerez, M. Álvarez-Láinez, J. M. Lagaron, *Coatings* **2018**, *8*, 173.
[63] D.-G. Yu, X.-L. Zheng, Y. Yang, X.-Y. Li, G. R. Williams, M. Zhao, *Appl. Surf. Sci.* **2019**, *473*, 148.
[64] J. Tian, Q. Ma, W. Yu, D. Li, X. Dong, G. Liu, H. Yu, *J. Phys. D: Appl. Phys.* **2020**, *53*, 155301.
[65] R.-M. Huang, K. Feng, S.-F. Li, M.-H. Zong, H. Wu, S.-Y. Han, *J. Food Eng.* **2021**, *307*, 110650.
[66] H. E. Abdelhakim, A. Coupe, C. Tuleu, M. Edirisinghe, D. Q. M. Craig, *Pharmaceutics* **2021**, *13*, 1665.
[67] H. Chen, Y. Zhao, L. Jiang, *Chin. Sci. Bull.* **2009**, *54*, 3147.
[68] H. Chen, Y. Zhao, Y. Song, L. Jiang, *J. Am. Chem. Soc.* **2008**, *130*, 7800.
[69] Y. Li, Y. Si, X. Wang, B. Ding, G. Sun, G. Zheng, W. Luo, J. Yu, *Biosens. Bioelectron.* **2013**, *48*, 244.
[70] J. Zhang, A. Mensah, C. Narh, X. Hou, Y. Cai, H. Qiao, Q. Wei, *Ceram. Int.* **2020**, *46*, 3543.
[71] M. A. Busolo, S. Torres-Giner, C. Prieto, J. M. Lagaron, *Innovative Food Sci. Emerging Technol.* **2019**, *51*, 12.
[72] M. M. A. Shirazi, S. Bazgir, F. Meshkani, *J. Water Process Eng.* **2020**, *36*, 101315.
[73] J. Ahmed, R. K. Matharu, T. Shams, U. E. Illangakoon, M. Edirisinghe, *Macromol. Mater. Eng.* **2018**, *303*, 1700577.
[74] G.-Z. Yang, J.-J. Li, D.-G. Yu, M.-F. He, J.-H. Yang, G. R. Williams, *Acta Biomater.* **2017**, *53*, 233.
[75] G. Chen, Y. Xu, D.-G. Yu, D.-F. Zhang, N. P. Chatterton, K. N. White, *Chem. Commun.* **2015**, *51*, 4623.
[76] B. Sanchez-Vazquez, A. J. R. Amaral, D.-G. Yu, G. Pasparakis, G. R. Williams, *AAPS PharmSciTech* **2017**, *18*, 1460.
[77] D.-G. Yu, J.-J. Li, M. Zhang, G. R. Williams, *Chem. Commun.* **2017**, *53*, 4542.
[78] S.-M. Ji, A. P. Tiwari, H. J. Oh, H.-Y. Kim, *Colloids Surf., A* **2021**, *621*, 126564.
[79] Z. Zhang, H. Yan, S. Li, Y. Liu, P. Ran, W. Chen, X. Li, *Chem. Eng. J.* **2021**, *404*, 127073.
[80] F. Mou, C. Chen, J. Guan, D.-R. Chen, H. Jing, *Nanoscale* **2013**, *5*, 2055.
[81] J. Tian, Q. Ma, W. Yu, D. Li, X. Dong, G. Liu, J. Wang, *RSC Adv.* **2019**, *9*, 10679.
[82] H. Kuang, Y. Wang, Y. Shi, W. Yao, X. He, X. Liu, X. Mo, S. Lu, P. Zhang, *Biomaterials* **2020**, *259*, 120288.
[83] D. Jin, S. Wu, H. Kuang, P. Zhang, M. Yin, *Mater. Des.* **2021**, *198*, 109301.
[84] E. Korina, O. Stoilova, N. Manolova, I. Rashkov, *J. Environ. Chem. Eng.* **2018**, *6*, 2075.
[85] R. J. Devolder, H. Bae, J. Lee, H. Kong, *Adv. Mater.* **2011**, *23*, 3139.
[86] M. Spasova, O. Stoilova, N. Manolova, I. Rashkov, M. Naydenov, *Polymers* **2020**, *12*, 1384.
[87] S. Zhang, H. Liu, N. Tang, J. Ge, J. Yu, B. Ding, *Nat. Commun.* **2019**, http://doi.org/10.1038/s41467-019-09444-y.
[88] H. Liu, L. Liu, J. Yu, X. Yin, B. Ding, *Compos. Commun.* **2020**, *22*, 100493.
[89] D. Sun, C. Chang, S. Li, L. Lin, *Nano Lett.* **2006**, *6*, 839.
[90] D. George, A. Garcia, Q. Pham, M. R. Perez, J. Deng, M. T. Nguyen, T. Zhou, S. O. Martinez-Chapa, Y. Won, C. Liu, R. C. Lo, R. Ragan, M. Madou, *Microsyst. Nanoeng.* **2020**, *6*, 7.
[91] I. Liashenko, J. Rosell-Llompart, A. Cabot, *Nat. Commun.* **2020**, *11*, 1.
[92] S. Liu, L. Sun, H. Zhang, Q. Hu, Y. Wang, M. Ramalingam, *Int. J. Biol. Macromol.* **2021**, *166*, 1280.
[93] M. Parhizkar, P. J. T. Reardon, J. C. Knowles, R. J. Browning, E. Stride, R. B. Pedley, T. Grego, M. Edirisinghe, *Mater. Des.* **2017**, *126*, 73.
[94] S. Xie, Y. Zeng, *Ind. Eng. Chem. Res.* **2012**, *51*, 5336.
[95] G. Yan, H. Niu, T. Lin, in *Electrospinning: Nanofabrication and Applications*, Elsevier, Netherlands **2018**, pp. 219–247.
[96] C. Zhang, M.-W. Chang, Z. Ahmad, W. Hu, D. Zhao, J.-S. Li, *RSC Adv.* **2015**, *5*, 87919.
[97] P. Ryšánek, O. Benada, J. Tokarský, M. Syrový, P. Čapková, J. Pavlík, *Mater. Sci. Eng., C* **2019**, *105*, 110151.
[98] W. Yu, X. Li, J. He, Y. Chen, L. Qi, P. Yuan, K. Ou, F. Liu, Y. Zhou, X. Qin, *J. Colloid Interface Sci.* **2021**, *584*, 164.
[99] K. Wei, X. Y. Gu, E. Z. Chen, Y. Q. Wang, Z. Dai, Z. R. Zhu, S. Q. Kang, A. C. Wang, X. P. Gao, G. Z. Sun, X. J. Pan, J. Y. Zhou, E. Q. Xie, *J. Colloid Interface Sci.* **2021**, *583*, 24.
[100] W.-M. Chang, C.-C. Wang, C.-Y. Chen, *Electrochim. Acta* **2019**, *296*, 268.
[101] C.-Y. Huang, M.-H. Chang, *Int. J. Energy Res.* **2021**, *45*, 12968.
[102] G. T. V. Prabu, B. Dhurai, *Sci. Rep.* **2020**, *10*, 4302.
[103] W. Yang, H. Li, X. Chen, in *Electrospinning: Nanofabrication and Applications*, Elsevier, Netherlands **2019**, pp. 339–361.
[104] Y. Ibrahim, E. Hussein, M. Zagho, G. Abdo, A. Elzatahry, *Int. J. Mol. Sci.* **2019**, *20*, 2455.
[105] H. C. Nam, W. H. Park, *Int. J. Biol. Macromol.* **2020**, *157*, 734.
[106] D. Buivydiene, A. M. Todea, C. Asbach, E. Krugly, D. Martuzevicius, L. Kliucininkas, *J. Aerosol Sci.* **2021**, *154*, 105754.
[107] X. Hong, S. Mahalingam, M. Edirisinghe, *Macromol. Mater. Eng.* **2017**, *302*, 1600564.
[108] U. Eranka Illangakoon, S. Mahalingam, K. Wang, Y.-K. Cheong, E. Canales, G. G. Ren, E. Cloutman-Green, M. Edirisinghe, L. Ciric, *Mater. Sci. Eng., C* **2017**, *74*, 315.
[109] P. L. Heseltine, J. Ahmed, M. Edirisinghe, *Macromol. Mater. Eng.* **2018**, *303*, 1800218.
[110] H. Alenezi, M. E. Cam, M. Edirisinghe, *Appl. Phys. Rev.* **2021**, *8*, 041412.

Pedro Miguel Silva completed his Master's in biological engineering at the University of Minho in 2015. In 2018, he started his Ph.D. program that he is currently concluding at the Centre of Biological Engineering at the University of Minho and at the International Iberian Nanotechnology Laboratory in Braga. He has published 10 research articles in international peer-reviewed journals and participated in works presented at more than 10 international conferences. Pedro is currently conducting research regarding the use of novel technologies (e.g., EHDP) for the development of functional food ingredients from compounds extracted from food industry by-products.

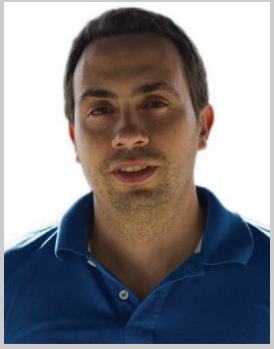

Sergio Torres-Giner holds a Dipl-Ing in chemical engineering, an M.Sc. in process systems technology, an MBA in industrial management, and a Ph.D. in food science. Since 2020, he works as a senior scientist at the Research Institute of Food Engineering for Development of the Polytechnic University of Valencia. Sergio does research in the field of macromolecular science of application interest in food packaging technology. He has more than 15 years of experience in both public research agencies and industrial R&D organizations. He has published more than 100 scientific articles, three books, 10 book and encyclopedia chapters, and four patents.

António Vicente is an associate professor with habilitation at the University of Minho since 2014 and vice-dean of the School of Engineering since 2019, following his previous appointment as Head of the Biological Engineering Department. He has been involved in 50 research projects, supervised 35 Ph.D. theses, 70 M.Sc. theses, and 20 post-doctoral fellows. António has published more than 350 research articles, five books, five patents, and 30 book chapters. He has been a Highly Cited Researcher (Clarivate Analytics – Agricultural Sciences) in 2018, 2019, 2020, and 2021, and received the Scientific Merit Prize of the University of Minho in 2021.

Miguel Cerqueira holds both a Graduation and Ph.D. degree in biological engineering from the University of Minho. He has authored more than 150 scientific articles, 20 book chapters, two patents, and is editor of three books. Miguel has supervised more than 15 students (Ph.D. and M.Sc.). In 2014, he won the Young Scientist Award and, in 2016, was selected as Inaugural Member of the International Academy of Food Science and Technology Early Career Scientist Section both organized by the International Union of Food Science and Technology. In 2018, he joined the Clarivate Highly Cited Researchers list.